Oxford Open Materials Science, 2021, 1(1): itab008

doi: 10.1093/oxfmat/itab008
Advance Access Publication Date: 7 June 2021
Review

REVIEW

Research progress in molecular dynamics simulation of CNT and graphene reinforced metal matrix composites

Changsheng Xing[1,‡], Jie Sheng[2,‡], Lidong Wang [1,*] and Weidong Fei[1,3]

[1]School of Materials Science and Engineering, Harbin Institute of Technology, Harbin 150001, China, [2]Laboratory for Space Environment and Physical Science, Research Center of Basic Space Science, Harbin Institute of Technology, Harbin 150001, China and [3]State Key Laboratory of Advanced Welding and Joining, Harbin Institute of Technology, Harbin 150001, China

[‡]Changsheng Xing and Jie Sheng contributed equally to this work.
*Correspondence address. School of Materials Science and Engineering, Harbin Institute of Technology, Harbin 150001, China. Tel: 86-0451-86418647; E-mail: wld@hit.edu.cn (L.D.W.)

ABSTRACT

Carbon nanomaterials are considered as one of the ideal choices for high-performance metal matrix composite reinforcements and one of the key directions of scientific research in recent years. Molecular dynamics simulation could be used conveniently to construct different composite material systems and study the properties of carbon nanomaterials reinforced metal matrix composites under different conditions. This review mainly introduces the molecular dynamic research progress of carbon nanotube (CNT) and graphene-reinforced metal (Cu, Al, Ni) composites. The potential functions of the carbon nanomaterials reinforced metal matrix composite simulation systems are briefly introduced. The dependence of the mechanical properties of metal matrix composites on the sizes, volume fraction and distribution states of CNT and graphene is detailed and discussed. Finally, we briefly summarize the future development direction of the molecular dynamic simulation with respect to carbon nanomaterials reinforced metal matrix composites.

Key words: carbon nanotube; graphene; microstructure; metal matrix composites; molecular dynamics; mechanical properties.

INTRODUCTION

In recent decades, new carbon nanomaterials [1] and graphene [2–5] have received extensive attention because of their excellent mechanical as well as physical properties. Carbon nanomaterials as reinforcements for metal matrix composites (such as Cu [6–14], Al [15–25], Ni [26–32]) have always been one of the key directions of scientific research. A series of studies show that the addition of a small amount of carbon nanomaterials will significantly improve the mechanical properties of metal matrix composites [33–45]. However, the reinforcement mechanism of carbon nanomaterials in metal composites is still far from well understood [46, 47]. The distribution of carbon nanomaterials, processing technology and interface bonding could have great impact on the comprehensive properties of composite materials [48]. To study these issues by experiments requires a long

Submitted: 10 February 2021; **Revised:** 13 May 2021; **Accepted:** 18 May 2021

experimental period and expensive experimental equipment, while molecular dynamics (MD) is a good way to solve these issues. MD simulation is one of the most effective methods for studying complex nanomaterial systems and has been widely used by many scholars in materials, mechanics, biology, physics, chemistry and other fields [49–53].

Recently, there have been a large number of reports using MD methods to study carbon nanotube (CNT) [54–58] and graphene reinforced metal composite materials [59–61]. MD could be used to study the reinforcing effect of CNT [62–65] and graphene [39, 66–68] with different structures on the properties of the metal matrix composites [69]. It is easy to apply tensile, compressive or indentation loads to the composite material system and the generation, proliferation and accumulation of dislocations in the simulated system can be directly observed with the visualization method, which is difficult to observe in actual experiments. This review mainly focuses on the influence of sizes, volume fraction and distribution states of CNT and graphene on the mechanical properties of metal matrix composites.

MD ON CARBON NANOMATERIALS REINFORCED METAL MATRIX COMPOSITES

Principles of MD simulation

MD simulation is a comprehensive technology that combines physics, mathematics, mechanics, chemistry and other disciplines [70–72]. It refers to a multibody system composed of atomic nuclei and electrons, based on the basic principles of Newtonian mechanics, using computers to simulate the motion process of atomic nuclei to analyze the structure and properties of the system. Currently, the most widely used open-source MD software is LAMMPS [72]. The force of each atom at any time is obtained through the interaction potential function between atoms, and classical Newtonian mechanics are used to calculate the speed and coordinates. And then the evolution of the model's microstructure, potential deformation mechanisms and other related properties can be studied.

One of the main advantages of MD simulation is that it is very convenient to observe the microscopic details of the system evolution by using the visualization method [73], which is difficult to observe in the experiment. At present, there are four main analysis methods to analyze the material structure: radial distribution function method [74], coordination number method [75], public nearest neighbor analysis method [76] and centrosymmetric parameter method [77]. The visual analysis software commonly used in MD simulation mainly includes ATOMEYE [78], VMD [79], OVITO [80] and so on. The combination of analytical methods and visual analysis software can reveal the evolution and deformation mechanism of the microstructure of carbon nanomaterials reinforced metal matrix composites.

Potential function

In MD simulation, the selection of potential function is very important because the potential function is used to describe the interaction between atoms (molecules) in the system. Whether the potential functions are used properly will directly affect the description of the observed physical/chemical event. Researchers usually choose different potential functions according to different research objects and environments. Even for the same research object, different potential functions need to be selected according to the different properties of the research. Below we introduce several common potential functions used in carbon nanomaterials reinforced metal matrix composites.

For carbon nanomaterials reinforced metal matrix composite system, the total energy of carbon nanomaterials reinforced metal matrix composites (E_{total}) usually consists of three parts:

$$E_{total} = E_{M-M} + E_{C-C} + E_{M-C} \quad (1)$$

where E_{M-M} and E_{C-C} describe the potential energies of the metal matrix and carbon nanomaterials, respectively, and E_{M-C} is the interaction between the metal and carbon atoms.

The interactions between the metal atoms (E_{M-M}) could be represented by the embedded-atom method (EAM) [81] or Morse potential [82]. For EAM [81], the total energy of the metal matrix system can be expressed as follows:

$$E^{EAM} = \sum_i F(\rho_i) + \frac{1}{2}\sum_{\substack{i,j \\ i \neq j}} \varphi_{ij}(R_{ij}) \quad (2)$$

$$\rho_i = \sum_{i \neq j} f(r_{ij})$$

where E^{EAM} is the total energy of the metal system, φ_{ij} represents the two-body central potential, R_{ij} represents the distance between different atoms i and j, $F(\rho_i)$ represents the embedded energy and ρ_i represents the electron cloud density of the ith atom.

For Morse potential [82], the total energy of the metal matrix system can be expressed as follows:

$$E^{Morse} = D0[e^{-2\alpha(rij-r0)} - 2e^{-\alpha(rij-r0)}] \quad (3)$$

where D_0 and α are the depth and width of the potential well, respectively, and r_0 is the interatomic distance at the equilibrium state.

The interactions between the carbon atoms (E_{C-C}) could be represented by the adaptive intermolecular reactive empirical bond order (AIREBO) potential [83] or Tersoff potential [84].

The AIREBO potential [83] consists of three items, namely the reactive empirical bond order (REBO) potential, the Lennard–Jones (LJ) potential, and the torsional interaction.

$$E^{AIREBO} = \frac{1}{2}\sum_i \sum_{j \neq i} [E_{ij}^{REBO} + E_{ij}^{LJ} + \sum_{k \neq i} \sum_{j \neq i,k} E_{kijl}^{Torsion}] \quad (4)$$

where E_{ij}^{REBO} represents the hydrocarbon REBO potential; E_{ij}^{LJ} represents the long-range interactions that are similar to LJ potential; $E_{kijl}^{Torsion}$ represents an explicit four-body potential that describes various dihedral angle preferences in the hydrocarbon configurations.

Tersoff potential [84] could be used to optimize the structures and calculate the energy of carbon nanomaterials. The equation is as follows:

$$E^{Tersoff} = \sum_i E_i = \frac{1}{2}\sum_{i \neq j} V_{ij} = \frac{1}{2}\sum_{i \neq j} f_c(r_{ij})[a_{ij} f_R(r_{ij}) + b_{ij} f_A(r_{ij})] \quad (5)$$

In this equation, E_i represents the potential of atom i, while f_R and f_A are the interactions of the repulsion and attraction between them. fc is the function of smooth section. $f_R(r_{ij})$ and $f_A(r_{ij})$

are presented as $Aexp(-\lambda r_{ij})$ and $-Bexp(-\mu r_{ij})$, respectively, a_{ij} and b_{ij} are the coefficients of repulsion and attraction, respectively [85].

The interactions between the metal atoms and carbon atoms (E_{M-C}) are usually described by the LJ potential which has been widely used to study the nanoscale materials and the obtained results coincide well with the experimental results [86–88]. The expression for the potential is as follows:

$$E^{LJ} = 4\varepsilon\left[\left(\frac{\sigma}{r_{ij}}\right)^{12} - \left(\frac{\sigma}{r_{ij}}\right)^{6}\right] \quad (6)$$

where E^{LJ} represents the potential energy between a pair of atoms, r_{ij} is the separation distance between the pair of atoms, ε is the depth of the potential well, and σ represents the van der Waals separation distance.

The interactions between the metal atoms and carbon atoms could also be described by the Morse potential [89, 90] and the ReaxFF Reactive Force Field [91]. The ReaxFF force field is used as it has been validated and tested successfully on different allotropic forms of carbon and even more importantly, can model the interactions between a few numbers of metal atoms like Ni and carbon atoms [92, 93].

MD SIMULATION ON CNT/METAL COMPOSITES

The influence of CNT layers, volume fraction and diameter on the mechanical properties of CNT/metal composites

The number of layers, volume fraction, diameter of CNTs in metal matrix composites have great impact on the mechanical properties of composites. MD simulation studies indicate that CNTs have an obvious reinforcing effect on metal matrix composites [58, 63, 94–97]. Figure 1a [95] exhibits the stress–strain behaviors of the single-walled CNTs (SWCNTs) reinforced copper matrix composites (SWCNTs/Cu). Compared with the pure copper, Young's modulus and yield strength of SWCNTs/Cu (8.6 vol.% SWCNTs) are increased by 33.92% (from 163.39 to 218.81 GPa) and 20.68% (from 8.77 to 10.58 GPa), respectively [95]. For 9 vol.% SWCNTs/Al, Young's modulus of the composite can be increased by 77% compared with pure Al. Even with a small amount (0.075 vol.%) of SWCNTs for SWCNTs/Cu, the mechanical properties of CNT/Cu composites could be significantly improved (~10–30%) [56]. The good reinforcement effect of the CNT in metal matrix composite is considered to be related to the high load-bearing capacity of CNTs because of their high strengths and surface areas [56, 98, 99].

The mechanical properties of CNT/metal composites could be improved by the increase of the tube layer number. Figure 1b [95] indicates the tensile stress–strain curves of SWCNTs/Cu, double-walled CNTs (DWCNTs)/Cu and triple-walled CNTs (TWCNTs)/Cu composites. According to the calculations, Young's modulus and yield strength of DWCNTs/Cu are 33.99 and 71.55% higher than SWCNTs/Cu. For TWCNTs/Cu, there are 72.3 and 172.68% improvement on these two performance indicators. As the number of layers increases, the strength and external surface area of CNT increase, the CNT in the composite can bear more stress transferred from the metal matrix [95].

The effects of CNT volume fraction on the mechanical properties of CNT/metal composites also have been studied [56, 95, 100, 101]. Figure 1c [95] shows that Young's modulus as well as yield strength of SWCNTs/Cu system increase with the volume fraction of SWCNTs (diameter = 20.34 Å). A linear relationship can be observed between the mechanical properties and the number of CNTs. With more amount of CNT, CNT/metal composites tend to present higher yield strength. Pal *et al.* [56] studied the effect of volume fraction on SWCNTs/Al composites (0–0.4 vol%), and similar conclusions were obtained. Young's modulus as well as the yield strength of SWCNTs/Al composites increases with the CNT volume fraction increasing from 0 to 0.4 vol%, as shown in Fig. 1d [56].

The diameter of CNTs is another factor that affects the mechanical properties of composite materials [63, 102]. Choi *et al.* [63] found that Young's modulus of (4,4)SWCNT/Al, (6,6)SWCNT/Al and (8,8)SWCNT/Al composites were 97.01, 99.02 and 103.3 GPa, respectively, improved by 31, 33 and 39%, compared with pure aluminum (74.24 GPa), as shown in Fig. 2a and b [63]. Patel *et al.* [101] studied the shear modulus of SWCNT/Al with different CNT diameters. They found that there was an optimal diameter for the shear modulus of CNT composites. The optimum diameter is 8.14 Å. When the diameter of CNTs is less than or greater than this value, it is not conducive to the improvement of the shear modulus of the composites. If the diameter of CNTs is too small, it is not conducive to play the role of reinforcement. If the diameter is too large, it will reduce the stability of the composite system and lead to the instability of the composite during deformation.

The effect of loading condition for the properties of CNT/metal composites

MD simulation studies demonstrated that the loading direction and the loading method for CNT/metal composite affected the mechanical properties of the composite [94, 99].

CNT parallel to the loading direction tends to have a better enhancement effect. Park *et al.* [99] found that the orientation of CNT could influence obviously the ultimate strength compared with the that of pure Al but affect Young's modulus not significantly. Figure 3a and b [99] shows the stress–strain curves with different CNT inclined degrees (0°, 10°, 20°, 30° and 40°). With the increase of the tilt of CNT, the ultimate strength decreased sharply from 7.3 to 4.3 GPa. For tilted CNTs, the strength decreased due to interface sliding and necking of the Al matrix. However, in the elastic region, the shapes of the stress–strain curve up to 0.05 strain are almost the same, corresponding to the same Young's modulus of 86 GPa.

Loading methods for CNT-metal composite also affect the mechanical properties of the composites. There are two loading methods acting on composites: loading only on the metal matrix (case A) and loading on both the metal matrix and CNT (case B). Silvestre *et al.* [65] used these two loading methods to study the mechanical properties of CNT/Al composites. Young's modulus in the case A (108 GPa) was increased by ~50%, and Young's modulus in the case B (142 GPa) was increased by 100%, compared with pure Al (71 GPa). These increases are not only due to the inherent stiffness of CNT, but also the contribution of interface sliding stress (~16 MPa for case A and 75 MPa for case B). Similarly, Faria *et al.* [103] studied the mechanical behavior of CNT/Cu composites with the two loading methods. The results show that when the load only acts on the Cu matrix (case A), the presence of CNT has an adverse effect on the tensile strength and compressive strength as well as the yield strain, and has no effect on elastic modulus. In case B, compared with pure Cu, Young's modulus of the CNT/Cu composite increases to 145 GPa (an increase of 32%); the presence of CNTs is

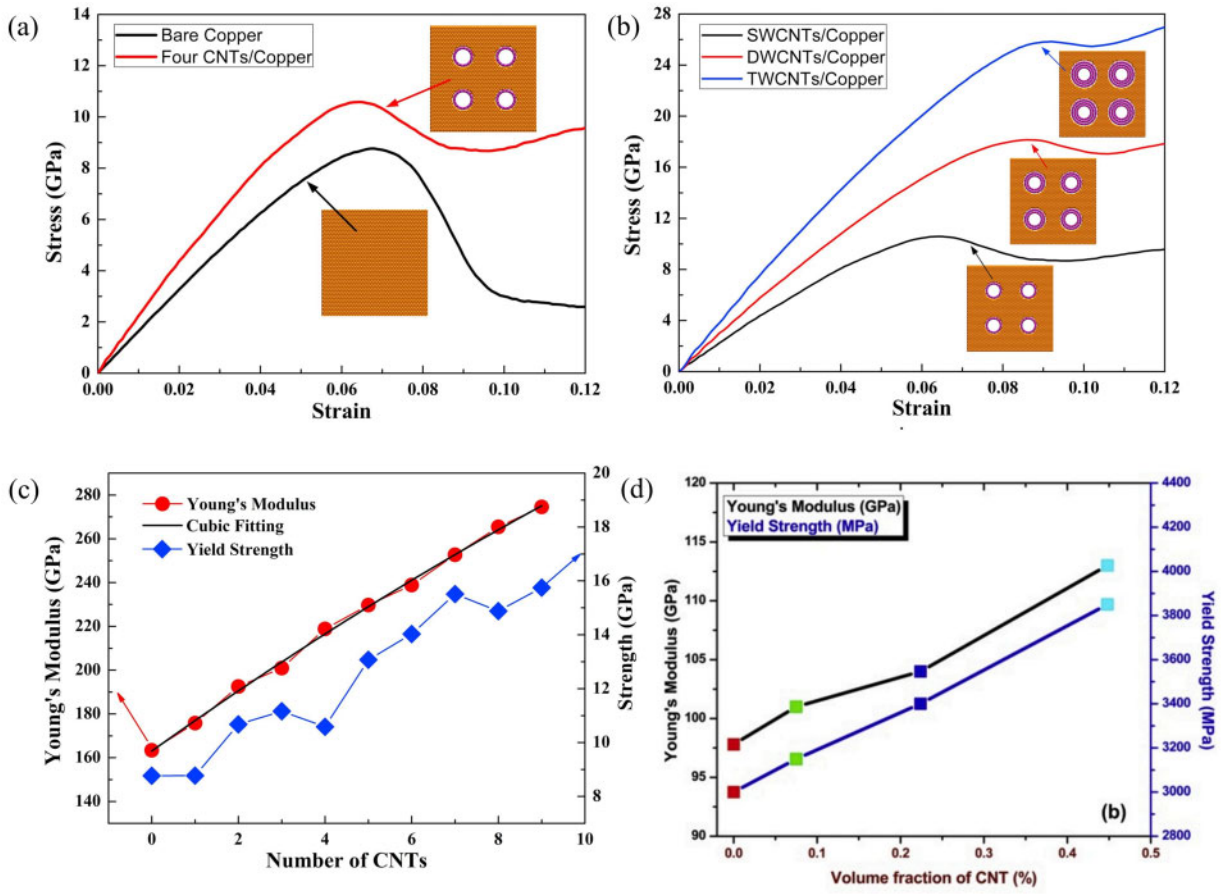

Figure 1: (a) The tensile stress–strain curves of CNTs/Cu and bare Cu [95]. (b) The stress–strain curves of different tube number CNTs/Cu composites [95]. (c) Young's modulus and yield strength of CNTs/Cu systems with different number of CNT [95]. (d) Mechanical properties for varying CNT volume fraction at 300 K [56]. Figures reproduced with permission from Ref. [95], Copyright 2018 Elsevier. Ref. [56], Copyright 2020 Elsevier.

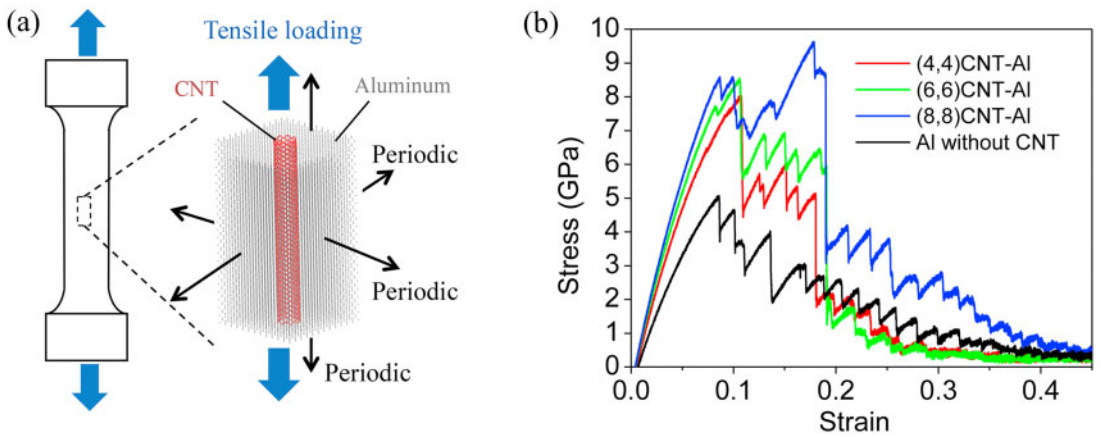

Figure 2: (a) Atomic model of CNT/Al composite specimen under tensile loading. (b) Stress–strain curves of CNT/Al composites with different CNT diameters [63]. Copyright 2016 Elsevier.

conducive to the improvement of tensile strength (14%) and compressive strength (66%), but reduces the yield (tensile and compressive) strain.

The interface of CNT/metal composites

Generally, there are two kinds of interfaces based on the interaction between CNTs and metal [104, 105]. One is strong conjunction interface, existing between CNT and Ni, Co; the other is weak conjunction interface (mainly Van der Waals interaction), existing between CNT and metal elements such as Cu and Al [106, 107].

For the weak conjunction interface, it is a significant method to enhance the interfacial strength by coating strong conjunction elements, such as Cr and Ni [108]. Duan *et al.* [109] studied

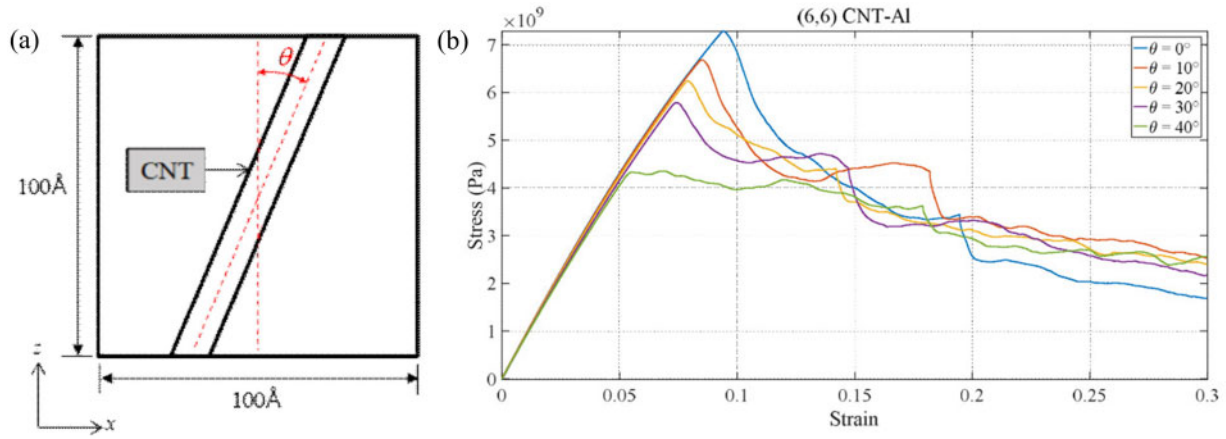

Figure 3: (**a**) Definition of CNT inclined degree and loading direction along the Z-axis. (**b**) The stress–strain curves of (6,6) CNT-Al with different CNT inclined degrees [99]. Copyright 2018 Springer Nature.

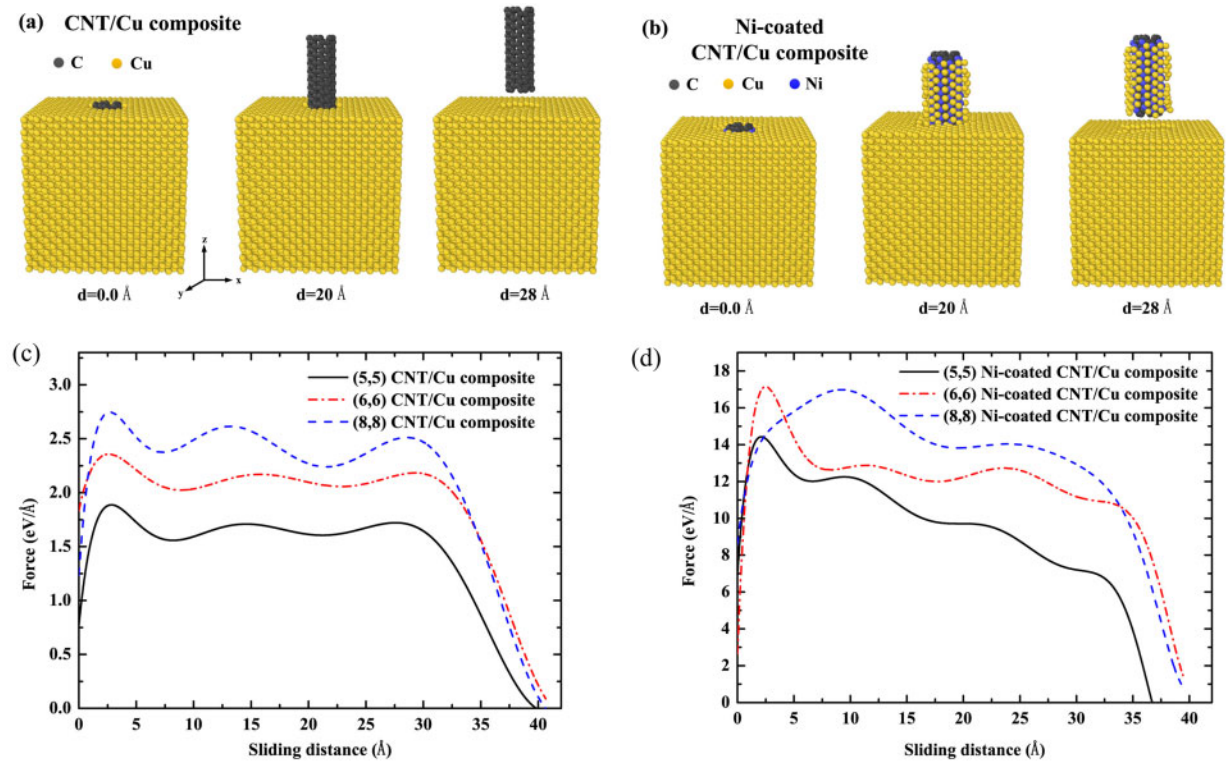

Figure 4: (**a**) Atomic model of CNT/Cu composite, (**b**) atomic model of Ni-coated CNT/Cu composite, (**c**) pullout force for CNT/Cu composites and (**d**) pullout force for Ni-coated CNT/Cu composite [109]. Figures reproduced with permission from Ref. [109]. Copyright 2017 Elsevier.

the drawing process of CNT in Ni-coated CNT/Cu composite. Atomic models of CNT/Cu composite and Ni-coated CNT/Cu composite are shown in Fig. 4a and b [109], respectively. Figure 4c and d [109] shows the pullout force for CNT/Cu and Ni-coated CNT/Cu composite. The results indicate that the interface strength of Ni-coated CNTs is significantly improved. Compared with the weak interaction between CNT and Cu, the addition of Ni improves the interaction between the two and improves the interface of the composite. In another work about Ni-coated CNT/Al composite [110], the results showed that the Ni-coated CNT may produce an extended interface ('interphase') between CNT and Al matrix, which will dissipate a large amount of energy during the CNT pullout process, resulting in a higher pullout force. Zhou *et al.* [111] studied the tensile process of Ni-coated CNT reinforced magnesium-based composites (Ni-CNT/Mg). The maximum stress of Ni-(6,6) CNT/Mg composite is 25.66% higher than the single-crystal Mg and 11.13% higher than uncoated (6,6) CNT/Mg composite. And the elastic modulus is increased by 23.69 and 14.43% compared with those two at 300 K.

GRAPHENE/METAL COMPOSITE MATERIALS

Graphene is regarded as one of the excellent reinforcements for metal matrix composites and there are many reports about graphene–metal composites [46, 47, 90, 112–115]. The focuses of

MD simulation researches are mainly on the influence of the microstructure of graphene and its distribution in the matrix on the properties of composites [116].

The influence of graphene layers, chirality and volume fraction on the mechanical properties of graphene/metal composites

The graphene layers, chirality have great influence on the reinforcement effect of the graphene/metal composites [116–118]. Duan *et al.* [119] investigated the mechanical properties of graphene nanoribbon embedded copper (GNR/Cu) composites and compared with pure Cu. Simulation models with different graphene layers and chirality are as shown in Fig. 5A [119]; the armchair and zigzag graphene nanoribbons are embedded between copper matrices. Figure 5B [119] shows the mechanical performance of GNR/Cu at various temperatures. Compared with single-crystal copper nanosheet, Young's modulus, tensile strength and breaking strain of GNR/Cu composites are much higher. For GNR/Cu composites, the number of graphene layers has a big impact on Young's modulus as well as tensile strength. Young's modulus of the single-layer GNR/Cu composites and the double-layer GNR/Cu composites are about 3 and 5 times of the pure Cu. The more the number of graphene layer, the greater the tensile strength of the composite.

Chirality of graphene has great effect on the tensile strength and strain of graphene/metal composites, but has little effect on their Young's modulus. As shown in Fig. 5B [119], the tensile strength (10.24 GPa at 300 K) of the single-layer zigzag graphene nanoribbon reinforced copper composite (SZGNR/Cu) is much larger than that (7.4 GPa at 300 K) of the single-layer armchair one (SAGNR/Cu), while their Young's moduli are not much different. Zhu *et al.* [120] also found that the chirality of graphene has an impact on the bending performance of graphene/Cu composite under three-point bending. The critical strain and force of the graphene/Cu composite in the zigzag direction are greater than these in the armchair direction. The zigzag graphene-embedded composites undergo a larger force than that in the armchair graphene because the magnitude of the bond angle variation in the zigzag direction is much larger than that in the armchair direction during the bending process [121].

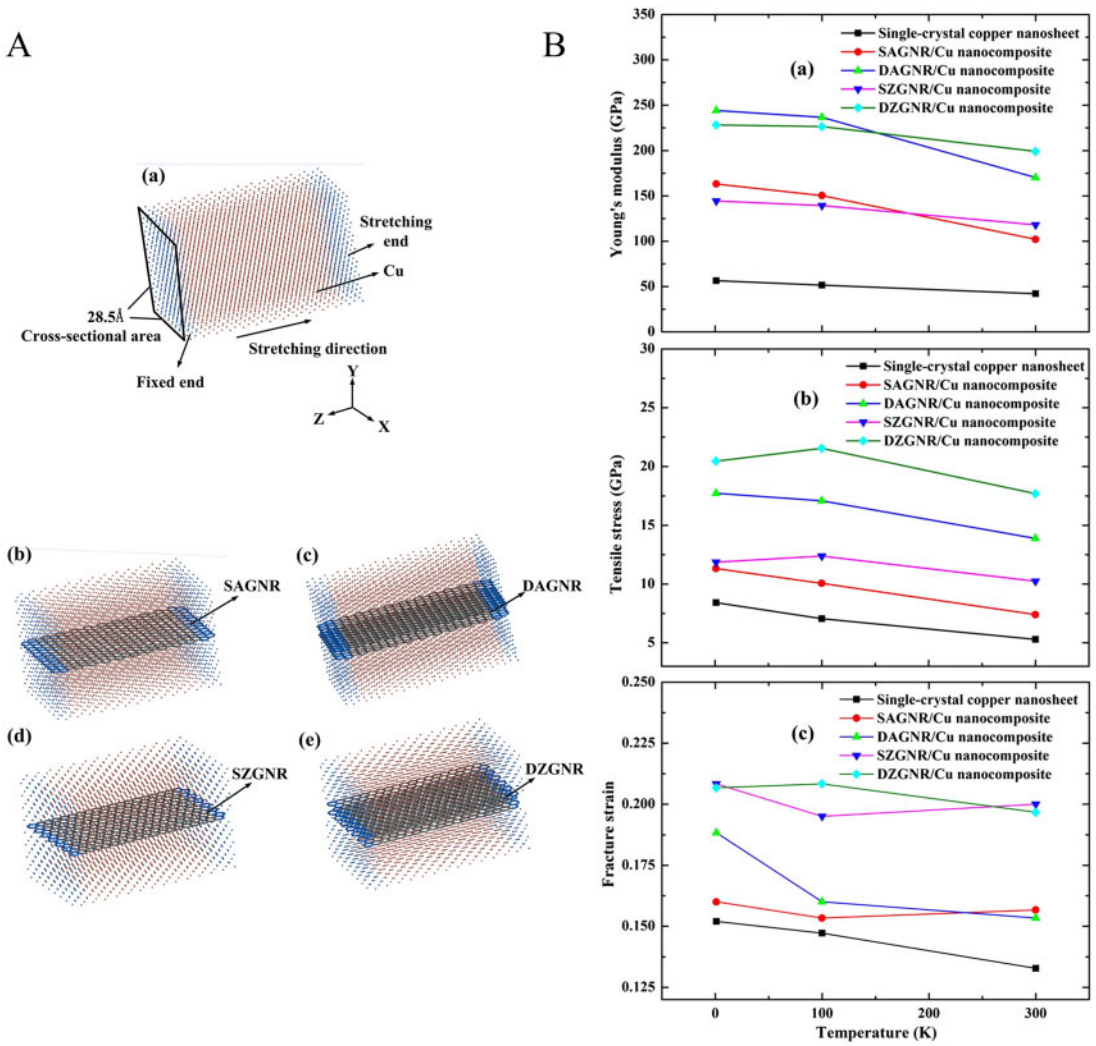

Figure 5: (**A**) Simulation models for the (**a**) perfect single-crystal copper nanosheet, (**b**) a single-layer armchair graphene nanoribbon copper composite (SAGNR/Cu), (**c**) double-layer armchair graphene nanoribbon copper composite (DAGNR/Cu), (**d**) a single-layer zigzag graphene nanoribbon copper composite (SZGNR/Cu) and (**e**) double-layer zigzag graphene nanoribbon copper composite (DZGNR/Cu). (**B**) Mechanical performance of the GNR/Cu composites at different temperatures [119]. Figures reproduced with permission from ref. [119]. Copyright 2016 Elsevier.

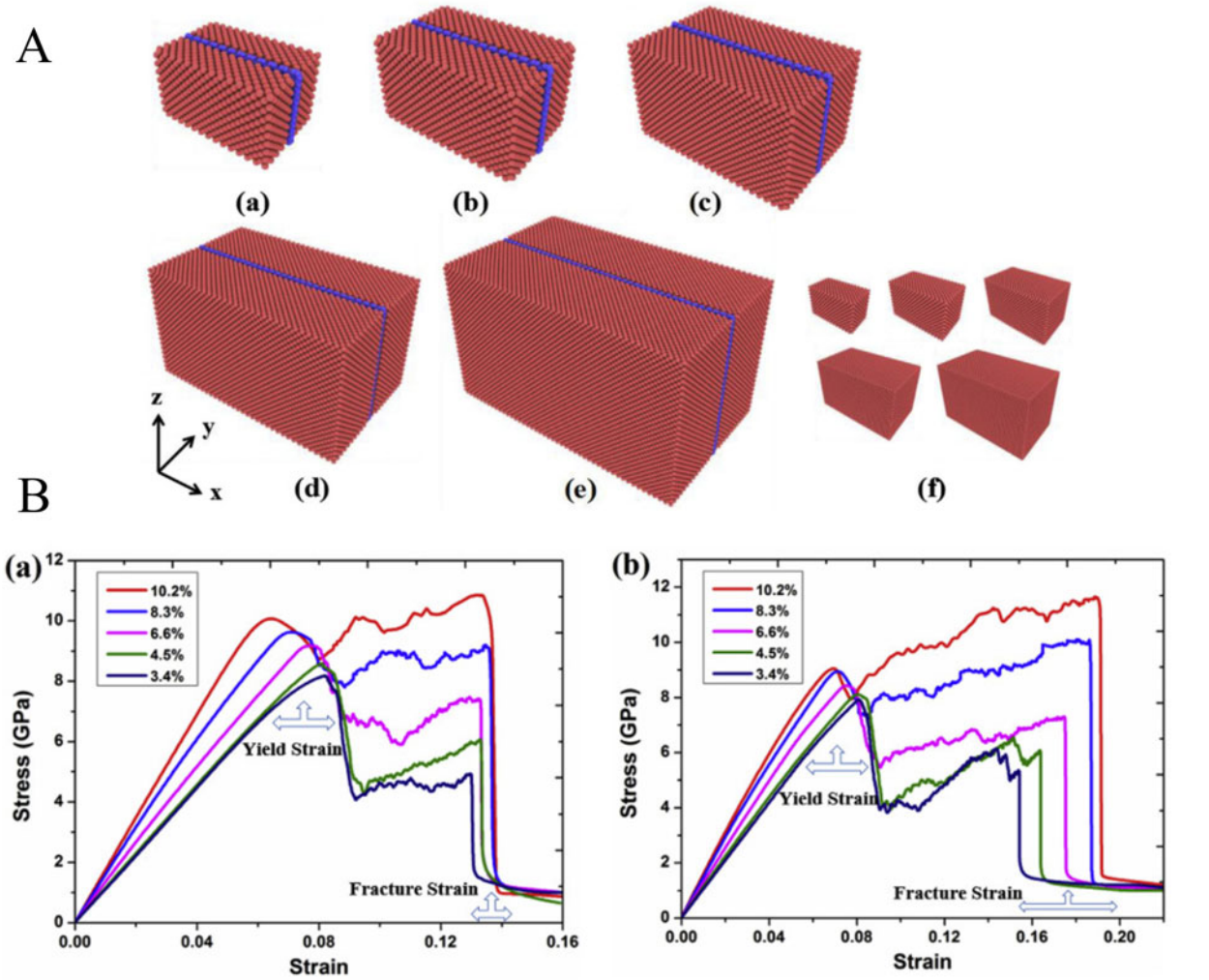

Figure 6: (**A**) Composites with different volume fraction of graphene: (**a**) 10.2 vol.%, (**b**) 8.3 vol.%, (**c**) 6.6 vol.%, (**d**) 4.5 vol.%, (**e**) 3.4 vol.% and (**f**) Pure copper; (**B**) stress–strain curves of the (**a**) armchair graphene/Cu and (**b**) zigzag graphene/Cu composites [122]. Figures reproduced with permission from Ref. [122]. Copyright 2016 Elsevier.

The volume fraction of graphene also plays an important role in mechanical properties of the graphene/metal composites. Zhang *et al.* [122] studied the influence of graphene volume fraction on the mechanical properties of graphene/Cu composites. As shown in Fig. 6A [122], the volume fractions of graphene in graphene/Cu composites were 3.4, 4.5, 6.6, 8.3 and 10.2 vol.%, and each model has a corresponding pure copper block as a comparison shown in Fig. 6A (f). Figure 6B [122] shows that the trend of each stress–strain curve has four regions: linear region, yield of matrix, fluctuation region and fracture region. First, the linear region corresponds to the elastic deformation stage of the graphene/Cu composite, in which the material deforms uniformly. Second, the composite reaches the maximum stress in the linear section, and the stress begins to drop suddenly, which corresponds to the yield of the composite. Third, under the synergistic effect of graphene and copper matrix, the stress of the composite fluctuates continuously because of dislocation slips, corresponding to the fluctuation region. Lastly, the stress suddenly drops directly to zero, which means the fracture of graphene. The increase of graphene volume fraction can significantly improve the mechanical property of the composites, which is related to the coordination of graphene and copper matrix. The 10.2 vol.% graphene/Cu composite has the maximum tensile strength with 11.65 GPa. Therefore, the increase of graphene volume fraction will improve the mechanical properties of composites.

The influence of arrangement structure on the mechanical properties of composites

The graphene layer spacing (λ) of the layered graphene–metal composite has an important influence on the performance of the composites [116, 123]. Zhang *et al.* [123] studied the role of λ in the shear deformation process of graphene/Cu composites as shown in Fig. 7. The value of shear failure stress (τ_F) of the composites increases as λ decreases. For $\lambda > 15$ nm, the τ_F value of polycrystalline graphene/Cu composites is close to or even smaller than that of monocrystalline Cu. When $\lambda \leq 15$ nm, the τ_F value of polycrystalline graphene/Cu composites is higher than that of monocrystalline Cu (~2.0 GPa at 300 K). Small λ affects the stability of the graphene/Cu composites, while large λ decreases their mechanical enhancement effect. Considering the yield, failure and interface stability, the optimal λ value of the composite is 2–15 nm. Within this optimal λ range, the

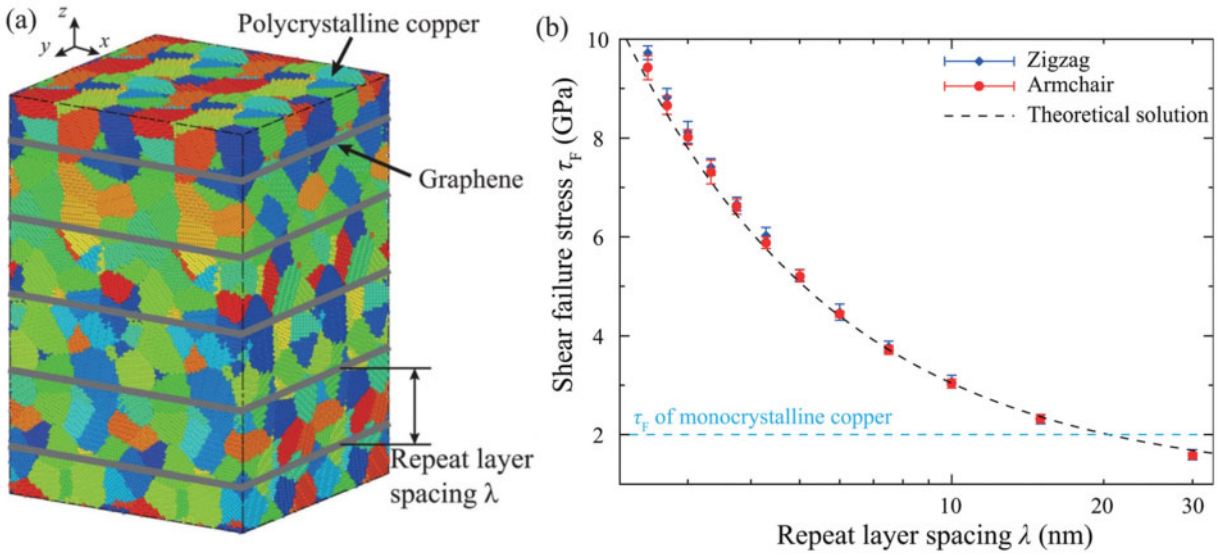

Figure 7: (**a**) Schematic of a polycrystalline copper–graphene composite. (**b**) Shear failure stress–repeat layer spacing (τ_F–λ) curves of polycrystalline copper-graphene composites [123]. Copyright 2018 The Royal Society of Chemistry.

composites can be designed by customizing the graphene/Cu interface, regardless of the microstructure of polycrystalline Cu.

The relationship between the direction of stress loading and the arrangement direction of graphene is another important issue [59, 124, 125]. Figure 8a–c depicts the stress–strain responses of pure Al and graphene/Al composites during tensile deformation along the *Z*-, *Y*- and *X*-axis [59]. Compared with pure Al (43.63 GPA), the stress–strain curve of tensile deformation along the *Z*-axis (70.96 GPA) shows significantly higher Young's modulus and yield strength. However, Young's modulus and yield strength are slightly higher than those of pure Al during tensile deformation along the *Y*- and *X*-axis. It demonstrates that the graphene sheets show reinforcing effect for the composite loading along the three directions, while the reinforcing effect along *Z*-axis is the best.

The influence of graphene/metal interface on the properties of composites

The interface interaction between graphene and metal matrix materials is usually an important factor that determines the mechanical properties of graphene/metal composites [126–129]. The graphene/metal interfaces could effectively prevent the metal atoms across the material. Although they are just a single layer of atoms in thickness, the matrix grains do not grow up easily, which is beneficial to the fine grain strengthening of the composite. Generally, there are two kinds of interface in graphene/metal composites: strong interaction interface and weak interaction interface. The strong interaction interface may occur due to (i) Carbides are formed at the graphene/metal interface. (ii) The graphene/metal interface has a small degree of atomic mismatch. (iii) The formation of large moire fringes. Weak interactions usually occur at the intersection of crystal grains [130].

For composites, the barrier effect of interface plays an important role in the interaction between graphene and metal matrix. During compressive loading process [131] or the cooling process [132] of graphene/metal composites, uneven interfaces of graphene and metal matrix are usually produced, which could limit the deformation of metal matrix and affect the properties of graphene/metal composites. Rezaei *et al.* [131] studied the deformation behavior of five metals (Cu, Ag, Au, Ni and Al)-graphene composites based on face-centered cubic metals under compressive loading. They found that deformation twinning can be achieved by limiting the movement of the metal atoms near the graphene layer, which introduces pseudoelasticity and shapes memory effects in a nanolayer film with a recoverable compressive strain of >15%. Zhou *et al.* [132] studied the generation of twisted grain boundaries and their influence on the mechanical properties of graphene/Al nanolayered composites by the MD methods. They found that the introduction of the graphene interface could affect the formation of twisted grain boundaries during the crystallization process. And the excellent load-bearing capacity of graphene interface plays an important role in the reinforcement of graphene/Al composites.

Graphene/metal interface also has an important influence on dislocations in composites [131, 133]. The interface in graphene–metal composites has two effects on the dislocations [134]. According to the dislocation density in the system, adding graphene to the metal matrix will improve or weaken the mechanical properties. When there are other defects in the matrix (such as grain boundaries in polycrystalline matrix), the interface will prevent the propagation of dislocations, which is caused by the defects in the matrix, and will improve the mechanical properties. However, if there is no dislocation in the metal matrix, the interface in the composite will act as the source of dislocation and weaken the material. Charleston *et al.* [133] used MD to simulate the influence of the graphene–nickel interface. They used graphene to enhance the perfect crystal of nickel and found that both the interface and graphene edges lead to reduced mechanical the strength of the composite. However, they added defects in the nickel-metal system and observed the improvement of mechanical properties of graphene/Ni composites. In the cylindrical system with defects, graphene improves the strength of the system significantly as shown in Fig. 9a [133]; Fig. 9b [133] shows the curves of dislocation density under different strains. It can be found that the dislocation density of the composite with seven graphene layers is almost the lowest among these samples at different stains. Figure 9c [133] shows the state of dislocations at 8% strain. The dislocation density of these composites decreases with the increase of

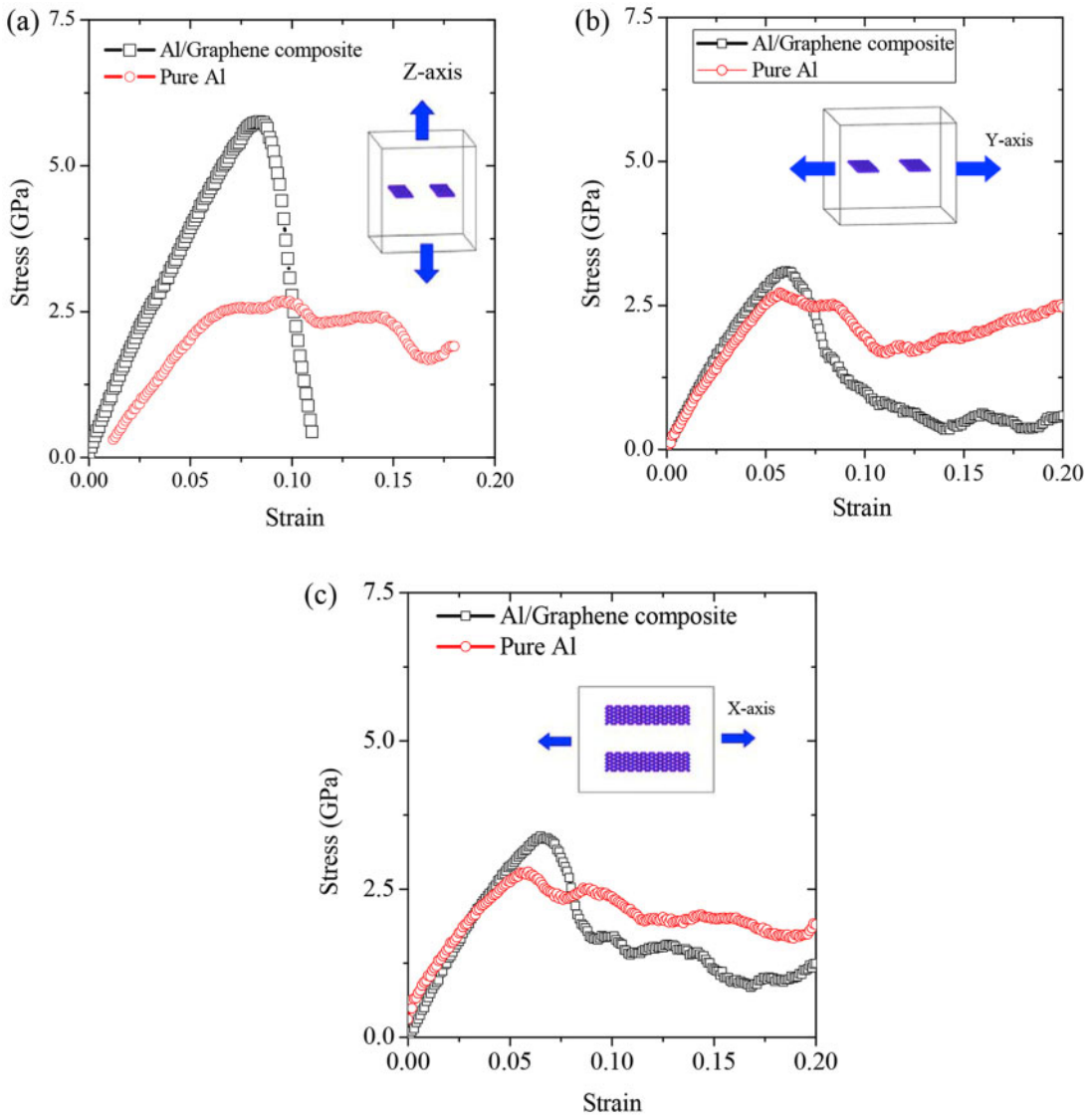

Figure 8: The stress–strain curves of pure Al and graphene/Al composite along: **(a)** Z-axis, **(b)** Y-axis and **(c)** X-axis [59]. Copyright 2018 Elsevier.

graphene layers, and for the composite with seven graphene layers, the dislocation density is near zero between the layers in the middle of the composite. The lower dislocation density is mainly caused by the effect of the interface as a termination of dislocations. The phenomenon of reduced dislocation density between graphene is called self-healing. The self-healing ability depends on the interlayer distance between graphene layers. Combining the enhancement and self-healing effects, the best distance between the single-layer graphene and the copper matrix is 5–15 nm [116]. Long *et al.* [135] found that the graphene/copper (111) interface hindered the diffusion of dislocations. During their study, no direct transfer of dislocations across graphene was observed. In another study, Hwang *et al.* [136] tested the bending fatigue of graphene/Cu composites with repeated interlayer spacing of 100 nm at 1.6% strain and 3.1% strain, up to 1 000 000 cycles. They found that fatigue cracks generated within the Cu layer were stopped by the graphene interface. The results also prove that the accumulation of dislocations at the graphene substrate interface has a self-healing phenomenon, which makes it difficult to form fatigue cracks in the composite system and propagate through graphene.

Nickel atoms at the interface between graphene and metal can also improve the mechanical properties of the composite. Montazeri *et al.* [137] used MD simulation to study the effect of Ni coating on the load transfer problem that occurs in the interface region of graphene/Cu composites. Under various amounts of 50, 75 and 100% nickel coating graphene, the average interfacial shear stress in the graphene/Cu composites can be increased to 99, 458 and 707%, respectively. Han *et al.* [138] studied the effect of Ni coating on Young's modulus of the graphene/Al composites. Their results also show that Young's modulus of pure Al can be effectively improved by inserting graphene coated with Ni, because the presence of Ni atoms improves the interface bonding and enables the load transfer capability of graphene to be exerted.

The effect of graphene functional groups on the properties of composites also has been studied [139–141]. The grafted functional groups on the surface of graphene can effectively increase the roughness of graphene, increase the contact area with the metal matrix, and thereby improve the mechanical properties of the composite material [139]. Zhao *et al.* [142] investigated the interfacial shear strength of graphene/Cu

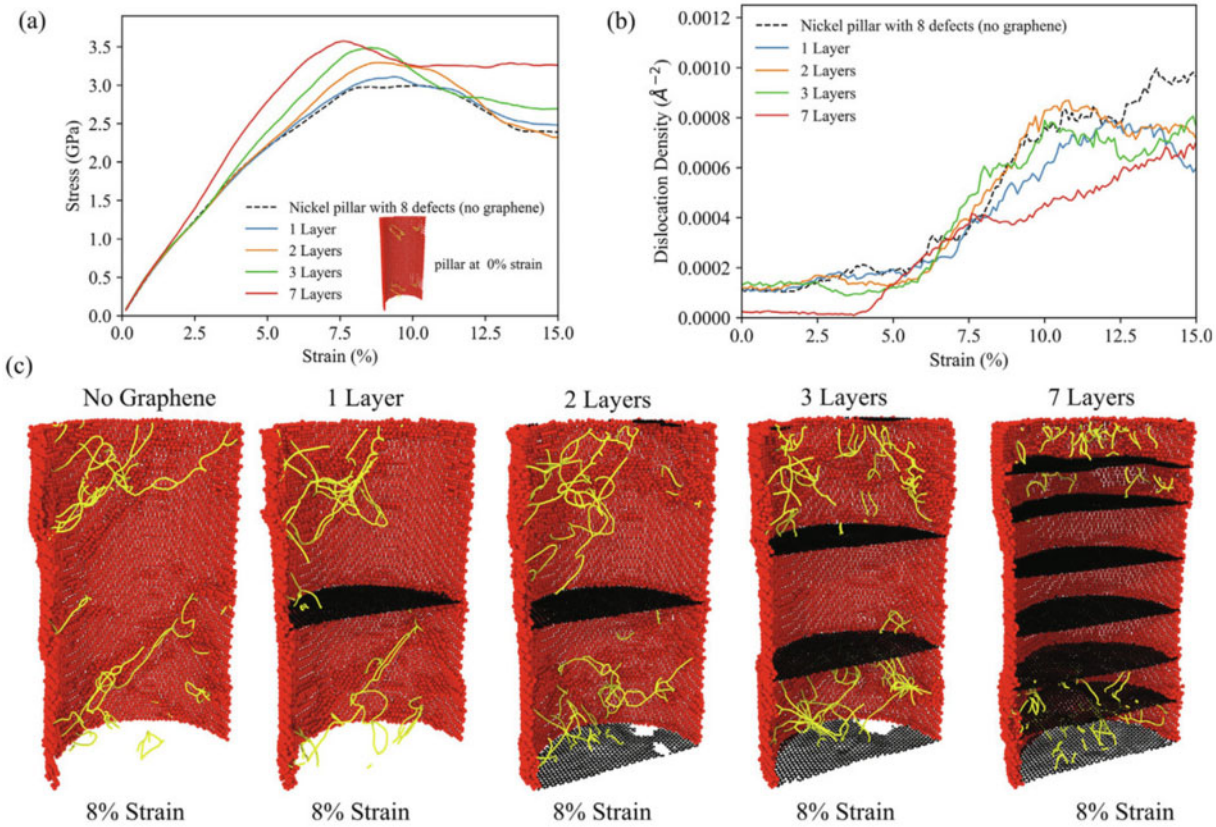

Figure 9: (**a**) The stress–strain curves of Ni columns with compression defects. (**b**) Dislocation density–strain curve for the same graphene–nickel configurations. (**c**) The dislocation state at 8% strain [133]. Copyright 2020 Elsevier.

composites. Their results show that the functional groups in graphene can significantly improve the interfacial shear strength of graphene/Cu composites. The average interfacial shear strength of 1% functionalized (C_4H_9) graphene/Cu composite is 386.0 MPa (101.5% higher than that without functionalization composite). Among the functional groups considered in the study, alkyl functionalization of graphene provides better interfacial shear strength than hydrogen functional groups because these are longer and can be more deeply embedded in the matrix than hydrogen functional groups.

The reinforcement mechanism of graphene/metal composites

The combination of MD simulations and visualization could be used to study the main strengthening mechanisms of graphene metal composites, such as the stress transfer, dislocation strengthening and structural enhancement, for different mechanical measurement methods [143, 144].

Stress transfer

Peng *et al.* [145] conducted an MD simulation of nanoindentation to study the effect of graphene on Cu plastic deformation under different indentation conditions. Figure 10a [145] shows an MD simulation model for indentation of Cu substrate with a single-layer graphene coating. Compared with bare copper substrate, the critical loads of single, double and triple graphene coatings increased by 114, 204 and 344%, respectively, as shown in Fig. 10b [143]. That means the presence and thickening of the graphene coating can improve the load-bearing capability of Cu substrate in the plastic stage [90, 145, 146]. The strengthening mechanism of the elastic phase is mainly the stress homogenization effect. Moreover, the graphene enhancement efficiency in the plastic stage is much higher than that in the elastic stage. The interaction between the dislocation and the graphene coating interface results in the enhancement of the graphene/Cu system in the plastic phase.

Similarly, Lei *et al.* [147] studied the nanoindentation response of the graphene/Al system. The results showed that the graphene layer expanded the bearing area by ∼5.36 times and changed the deformation behavior of the Al substrate during the nanoindentation process. Compared with the pure Al system, the load-bearing capacity of the graphene/Al system was significantly increased by ∼4.7 times. And the enhancement effect of double-layer graphene was ∼1.5 times that of single-layer graphene. The indentation mechanical properties of multilayer graphene on Ni were also studied [148]. The critical loads of graphene fracture from single layer to four-layer graphene are 1104, 1776, 2210 and 3176 nN, respectively. Compared with the single graphene/Ni system, the bearing capacity of the system increased by 60.9, 100.1 and 187.7% when the number of layers increased to 2, 3 and 4, respectively. Yang *et al.* [149] simulated the plastic deformation and fracture behavior of graphene/nickel composites. It is found that the strength and ductility of the metal matrix can be greatly improved by adding graphene. They also found that sliding at the interface released the stress in the graphene layer, resulting in a more uniform stress distribution on the graphene.

The stress transfer effect of graphene is also related to the coverage percent of graphene on metal grain [150]. Figure 11A

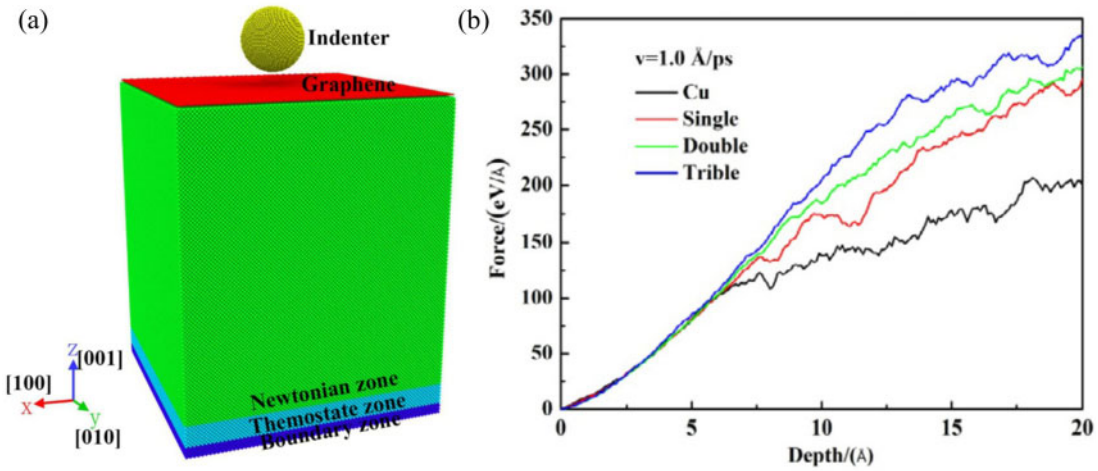

Figure 10: (**a**) A MD simulation model for indentation of Cu substrate with a single-layer graphene coating. (**b**) The typical load–depth curves of displacement-controlled indentation [145]. Figures reproduced with permission from Ref. [145], Copyright 2019 Elsevier.

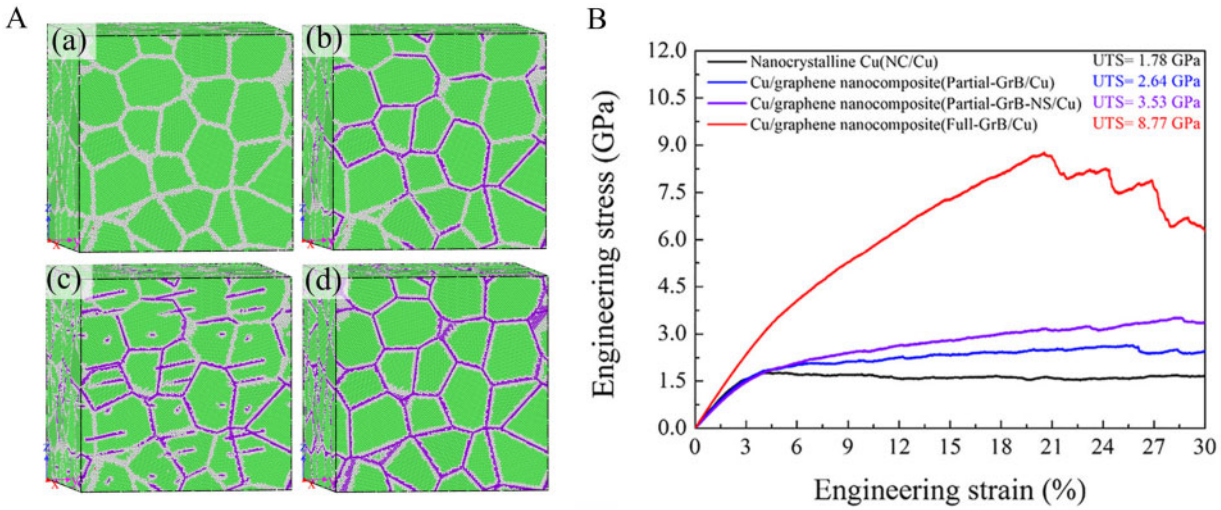

Figure 11: (**a**) The 3D models of graphene/Cu composite with different graphene coverage percent. (**b**) The stress–strain curves of tensile deformation [150]. Figures reproduced with permission from Ref. [150], Copyright 2020 Elsevier.

(a–d) [150] shows the detailed 3D models of graphene/Cu composite with different graphene coverage percent. The proportion of graphene-coated crystal boundaries increases gradually and Fig. 11B shows the engineering stress–strain curves of these models [150]. It can be seen from the results, the composites with fully coated grain boundaries have the highest strain hardening rate and tensile strength. Its tensile strength reaches 8.77 GPa, which is about 5 times higher than that of nanocrystalline Cu (no graphene embedded) and 3 times higher than that of graphene/Cu composite partially enclosed by graphene boundaries (9.1 vol.%). Their research results show that as the coverage percent increases, more graphene can bear more stress from grain boundaries.

Dislocation strengthening

The dislocation strengthening in graphene/metal composite is mainly caused by dislocation stacking, dislocation winding and dislocation patterns [151–154]. Because graphene is currently the highest tensile strength material, its hindering effect of dislocations is very significant. Zhu *et al.* [152] studied the effect of graphene layers on the movement of dislocations in the Al matrix. In the simulation, they found that the graphene sheets in the graphene/Al composite limit the slip of dislocations, resulting in an increase of dislocation density at the interface as shown in Fig. 12 [152]. The high dislocation density at the graphene interface enhances the strength of the graphene/Al composite. Dislocation transmission across graphene is very difficult due to the high energy barrier required to cause the in-plane deformation of graphene, which allowed the graphene mechanical properties to affect the dislocation strengthening [155].

The dislocation strengthening is also related to the orientations of the metal crystal. Figure 13 [152] shows the stress–strain curves for the pure Al and graphene/Al composites with three crystal orientations. For each direction, the strength of the composite is higher than that of the corresponding Al matrix, reflecting the strengthening effect of graphene. The dislocation densities for graphene/Al with [1 1 0] direction is much higher than those in other directions. As a result, this composite exhibits the highest tensile strength, which indicates that the mechanical properties of the graphene/Al composites are affected by the crystal direction.

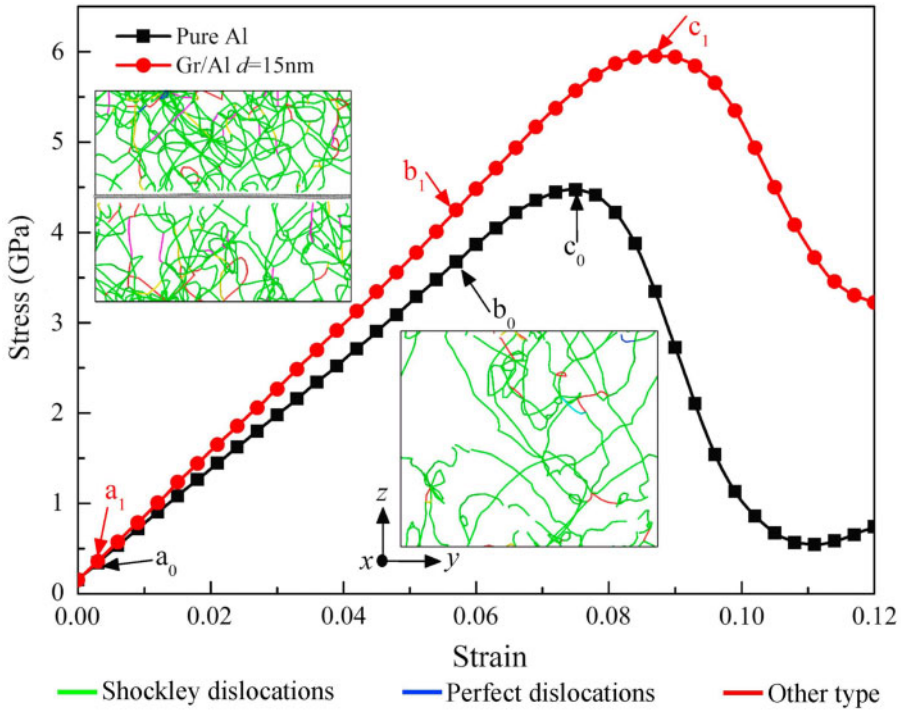

Figure 12: Stress–strain curves of the Al and graphene/Al composite and dislocation analysis [152]. Copyright 2019 Elsevier.

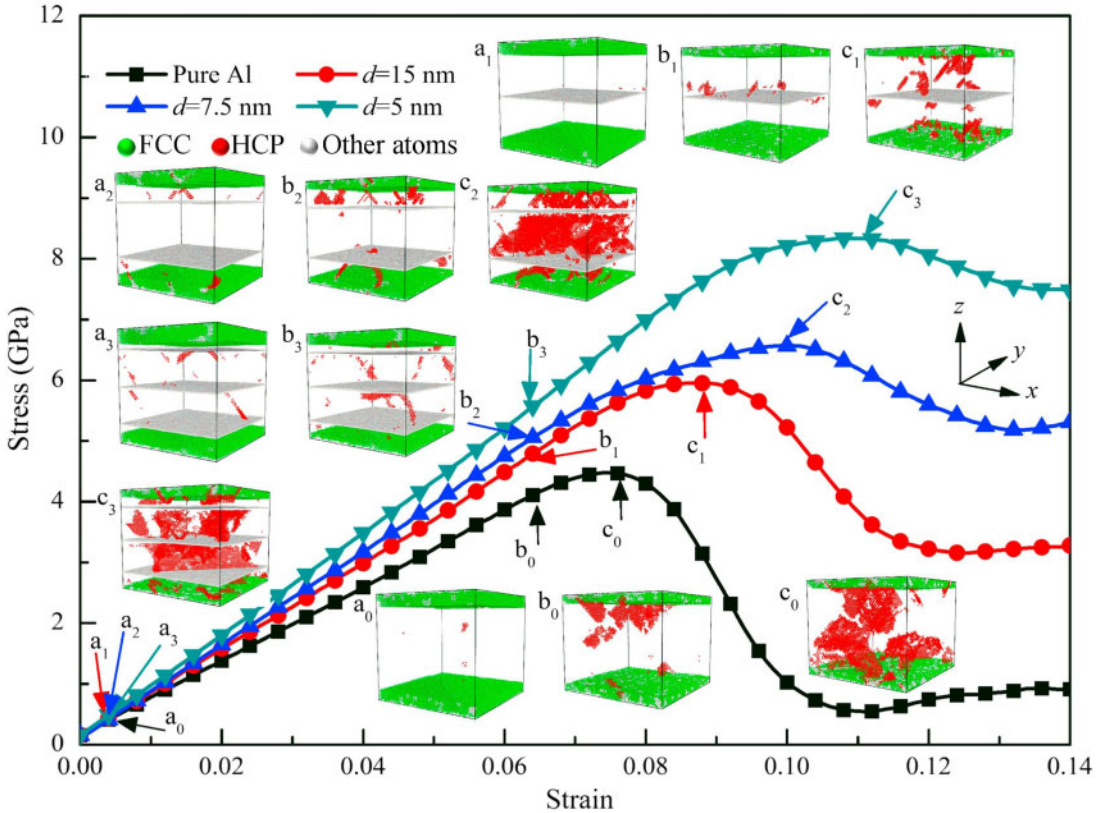

Figure 13: Stress–strain curves for the pure Al and graphene/Al composites with three different crystal orientations, and the development of their interior dislocation nucleation [152]. Copyright 2019 Elsevier.

Structural enhancement

The structure is another factor that can significantly affect the enhancement effect of graphene [156, 157]. Zhang *et al.* [156] studied the difference in enhancement effect between 2D and 3D graphene. Figure 14a and b shows the model of 2D- and 3D-graphene sheet embedded in a copper block. The force and

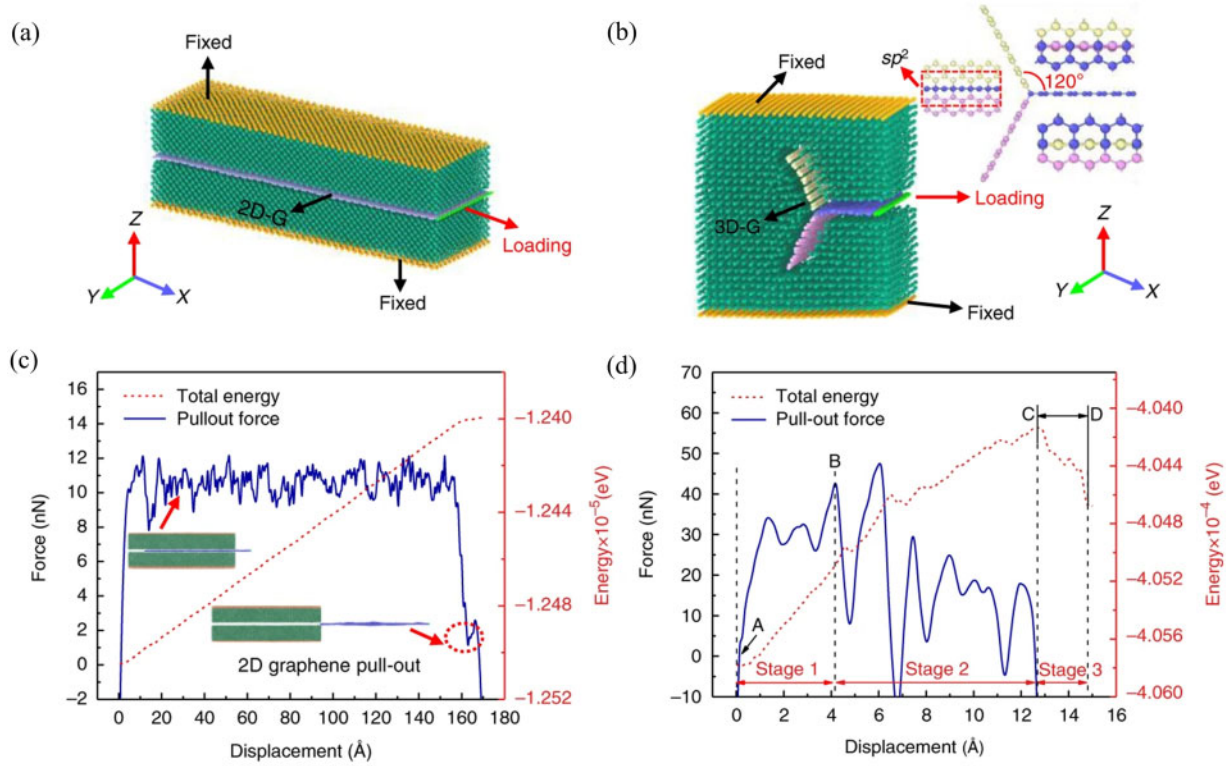

Figure 14: Atomic models in MD simulations of **(a)** 2D-graphene/Cu and **(b)** 3D-graphene/Cu. The simulated pull-out force-displacement curves of **(c)** 2D-graphene/Cu and **(d)** 3D-graphene/Cu [156]. Copyright 2020 Springer Nature.

displacement corresponding to the process of pulling out the graphene from the two models are presented in Fig. 14c and d, respectively. The average pull-out force of 3D graphene is significantly higher than that of 2D graphene, which is attributed to the enhanced structure of graphene. The structural enhancement of graphene mainly plays a role in three aspects. First, the continuous 3D-graphene structure can hinder the growth of crystal grains, thus leading to fine-grain strengthening. Second, the 3D structure introduces more interfaces inside the composite material, which can more effectively prevent dislocations from crossing the grain boundaries. Third, 3D graphene has a better load transfer effect [156].

Comparison of the enhancement effect of CNT and graphene

The contrast between the enhancement effect of CNT and graphene is focus of the researchers. Ke Duan *et al.* [158] studied the interface properties of graphene/Cu and CNT/Cu composites. They found that both the total energy and pull-out force of graphene/Cu composites are higher than those of CNT/Cu composites as shown in Fig. 15a and b [158]. In the same state, graphene layers have a greater interaction force than CNT with the metal matrix. Compared with CNT, graphene layers have better load transfer ability, because of the unique 2D layered structure of graphene. In addition, their dispersion in the metal matrix is easier than CNT, making them a good candidate as metal-strengthening nanocarrier.

A series of MD simulations were designed to evaluate the enhancement effect of CNT and graphene [159, 160]. Under the same conditions, two different calculation units were compared, namely, graphene/Cu and CNT/Cu samples [160]. At 5 vol.%, Young's modulus of the graphene/Cu composite was 58.9% higher than the pure copper. Meanwhile, CNT showed only a 35.5% increase in the copper modulus for the same volume fraction. Sharma *et al.* [159] also studied the difference of thermal conductivity between the graphene/Cu and CNT/Cu composites. Their results show that with the increase of nanofiller volume fraction, the thermal conductivity of the graphene/Cu composite increases at a faster rate than the CNT/Cu composite. The above results all indicate that graphene has a better enhancement effect than CNT in their studies.

CONCLUSIONS AND PROSPECTS

This article mainly introduces the recent progress in MD research on CNT and graphene reinforced metal matrix composites (Cu, Al, Ni). A series of MD simulation results revealed the reinforcing effect of CNT and graphene on the metal matrix at the atomic or molecular level. The shapes, sizes, volume fraction and distributions of CNT and graphene have comprehensive effects on the performances of metal matrix composites. By using visualization software, researchers can easily observe the effects of carbon nanomaterials in different states in the metal matrix and study the mechanical properties, the generation and slipping process of dislocations and enhancement mechanisms of the CNT and graphene reinforced metal composites.

Although the MD research on carbon nanomaterials reinforced metal matrix composites has made great progress, there are still several challenges to be overcome. First, the graphene and CNTs with perfect crystal quality are generally used in the composites, which result in the difference between MD simulation and experimental results. Second, the electrical and thermal conductivities of carbon nanomaterials reinforced metal matrix composites are less investigated and scarcely reported

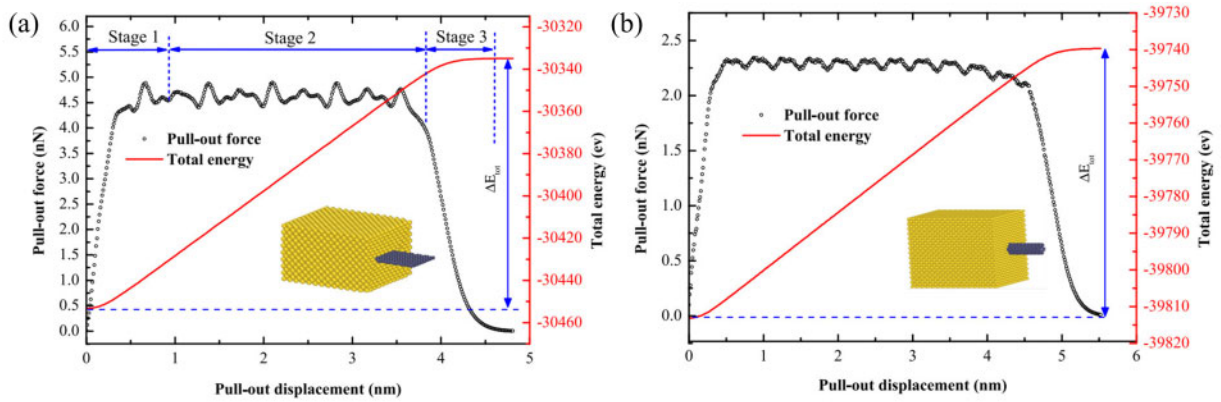

Figure 15: The curves of total energy and pull-out force as a function of pull-out distance for the case of (**a**) graphene/Cu composites and (**b**) CNT/Cu composites [158]. Copyright 2017 IOP Publishing.

compared with mechanical properties because of the lack of suitable algorithms and potential functions. Third, to obtain simulation results consistent with actual experiments, increasing the number of atoms in the simulation system is an effective solution, while a large simulation system has higher requirements on the computing resources. In the future, artificial intelligence techniques would play an important role in MD simulations by increasing the accuracy of potential functions, optimizing algorithm and improving calculation speed. For example, machine learning is being used to choose materials for a specific intention through Materials Project [161–163]. In addition, MD simulations could be combined with the density functional theory and the finite element method to provide simulation results closer to the actual performance. Consequently, MD simulations could provide beneficial references for actual scientific research, and help researchers study and develop new materials more conveniently in the future.

ACKNOWLEDGEMENTS

The authors gratefully acknowledge the support from National Natural Science Foundation of China (Grant no. 51671069 and No. 51801043), The Fundamental Research Funds for the Central Universities (Grant no. ZDXMPY20180104), State Administration of Science Technology and Industry for National Defense (Grant no. JCKYS2019603C017) and the China Postdoctoral Science Foundation (Grant no. 2019M650065).

CONFLICT OF INTEREST STATEMENT

The authors declare no conflict of interest

REFERENCES

1. De Volder MFL, Tawfick SH, Baughman RH et al. Carbon nanotubes: present and future commercial applications. *Science* 2013;**339**:535–39.
2. Geim AK, Novoselov KS. The rise of graphene. *Nat Mater* 2007;**6**:183–91.
3. Novoselov KS, Geim AK, Morozov SV et al. Two-dimensional gas of massless Dirac fermions in graphene. *Nature* 2005; **438**:197–200.
4. Novoselov KS, Geim AK, Morozov SV et al. Electric field effect in atomically thin carbon films. *Science* 2004;**306**:666–69.
5. Stankovich S, Dikin DA, Dommett GHB et al. Graphene-based composite materials. *Nature* 2006;**442**:282–86.
6. Kim KT, Eckert J, Liu G et al. Influence of embedded-carbon nanotubes on the thermal properties of copper matrix nanocomposites processed by molecular-level mixing. *Scr Mater* 2011;**64**:181–84.
7. Kim KT, Il Cha S, Gemming T et al. The role of interfacial oxygen atoms in the enhanced mechanical properties of carbon-nanotube-reinforced metal matrix nanocomposites. *Small* 2008;**4**:1936–40.
8. Yoo SJ, Han SH, Kim WJ. A combination of ball milling and high-ratio differential speed rolling for synthesizing carbon nanotube/copper composites. *Carbon* 2013;**61**:487–500.
9. Chen F, Ying J, Wang Y et al. Effects of graphene content on the microstructure and properties of copper matrix composites. *Carbon* 2016;**96**:836–42.
10. Chu K, Wang X-H, Wang F et al. Largely enhanced thermal conductivity of graphene/copper composites with highly aligned graphene network. *Carbon* 2018;**127**:102–12.
11. Hwang J, Yoon T, Jin SH et al. Enhanced mechanical properties of graphene/copper nanocomposites using a molecular-level mixing process. *Adv Mater* 2013;**25**:6724–29.
12. Kim WJ, Lee TJ, Han SH. Multi-layer graphene/copper composites: preparation using high-ratio differential speed rolling, microstructure and mechanical properties. *Carbon* 2014; **69**:55–65.
13. Shi Z, Sheng J, Yang Z et al. Facile synthesis of high-performance carbon nanosheet/Cu composites from copper formate. *Carbon* 2020;**165**:349–57.
14. Yang Z, Wang L, Shi Z et al. Preparation mechanism of hierarchical layered structure of graphene/copper composite with ultrahigh tensile strength. *Carbon* 2018;**127**:329–39.
15. Liu ZY, Xiao BL, Wang WG et al. Singly dispersed carbon nanotube/aluminum composites fabricated by powder metallurgy combined with friction stir processing. *Carbon* 2012; **50**:1843–52.
16. Liu ZY, Xu SJ, Xiao BL et al. Effect of ball-milling time on mechanical properties of carbon nanotubes reinforced aluminum matrix composites. *Compos Part A Appl Sci Manuf* 2012; **43**:2161–68.
17. Park JG, Keum DH, Lee YH. Strengthening mechanisms in carbon nanotube-reinforced aluminum composites. *Carbon* 2015;**95**:690–98.

18. Wang L, Choi H, Myoung J-M et al. Mechanical alloying of multi-walled carbon nanotubes and aluminum powders for the preparation of carbon/metal composites. *Carbon* 2009; **47**:3427–33.
19. Bartolucci SF, Paras J, Rafiee MA et al. Graphene-aluminum nanocomposites. *Mater Sci Eng A* 2011;**528**:7933–37.
20. Feng S, Guo Q, Li Z et al. Strengthening and toughening mechanisms in graphene-Al nanolaminated composite micro-pillars. *Acta Mater* 2017;**125**:98–108.
21. Li Z, Guo Q, Li Z et al. Enhanced mechanical properties of graphene (reduced graphene oxide)/aluminum composites with a bioinspired nanolaminated structure. *Nano Lett* 2015; **15**:8077–83.
22. Rashad M, Pan F, Tang A et al. Effect of graphene nanoplatelets addition on mechanical properties of pure aluminum using a semi-powder method. *Prog Nat Sci-Mater Int* 2014;**24**: 101–08.
23. Shin SE, Choi HJ, Shin JH et al. Strengthening behavior of few-layered graphene/aluminum composites. *Carbon* 2015; **82**:143–51.
24. Wang J, Li Z, Fan G et al. Reinforcement with graphene nanosheets in aluminum matrix composites. *Scr Mater* 2012;**66**: 594–97.
25. Zhou W, Yamaguchi T, Kikuchi K et al. Effectively enhanced load transfer by interfacial reactions in multi-walled carbon nanotube reinforced Al matrix composites. *Acta Mater* 2017; **125**:369–76.
26. Hwang JY, Lim BK, Tiley J et al. Interface analysis of ultrahigh strength carbon nanotube/nickel composites processed by molecular level mixing. *Carbon*, 2013. **57**: 282–87.
27. Sun Y, Sun J, Liu M et al. Mechanical strength of carbon nanotube-nickel nanocomposites. *Nanotechnology* 2007;**18**: 505704.
28. Uddin J, Baskes MI, Srinivasan SG et al. Modified embedded atom method study of the mechanical properties of carbon nanotube reinforced nickel composites. *Phys Rev B* 2010;**81**: 104103
29. Kuang D, Xu L, Liu L et al. Graphene-nickel composites. *Appl Surf Sci* 2013;**273**:484–90.
30. Mai YJ, Chen FX, Lian WQ et al. Preparation and tribological behavior of copper matrix composites reinforced with nickel nanoparticles anchored graphene nanosheets. *J Alloys Compd* 2018;**756**:1–7.
31. Tang Y, Yang X, Wang R et al. Enhancement of the mechanical properties of graphene-copper composites with graphene-nickel hybrids. *Mater Sci Eng A* 2014;**599**:247–54.
32. Yasin G, Khan MA, Arif M et al. Synthesis of spheres-like Ni/graphene nanocomposite as an efficient anti-corrosive coating; effect of graphene content on its morphology and mechanical properties. *J Alloys Compd* 2018;**755**:79–88.
33. Fu K, Zhang X, Shi C et al. An approach for fabricating Ni@graphene reinforced nickel matrix composites with enhanced mechanical properties. *Mater Sci Eng A* 2018;**715**: 108–16.
34. Jiang J, He X, Du J et al. In-situ fabrication of graphene-nickel matrix composites. *Mater Lett* 2018;**220**:178–81.
35. Ameri S, Sadeghian Z, Kazeminezhad I. Effect of CNT addition approach on the microstructure and properties of NiAl-CNT nanocomposites produced by mechanical alloying and spark plasma sintering. *Intermetallics* 2016;**76**: 41–48
36. Huang Z, Zheng Z, Zhao S et al. Copper matrix composites reinforced by aligned carbon nanotubes: mechanical and tribological properties. *Mater Des* 2017;**133**:570–78.
37. Bor A, Ichinkhorloo B, Uyanga B et al. Cu/CNT nanocomposite fabrication with different raw material properties using a planetary ball milling process. *Powder Technol* 2018;**323**: 563–73.
38. Cha SI, Kim KT, Arshad SN et al. Extraordinary strengthening effect of carbon nanotubes in metal-matrix nanocomposites processed by molecular-level mixing. *Adv Mater* 2005; **17**:1377.
39. Kim Y, Lee J, Yeom MS et al. Strengthening effect of single-atomic-layer graphene in metal-graphene nanolayered composites. *Nat Commun* 2013;**4**:2114.
40. Xiong D-B, Cao M, Guo Q et al. Graphene-and-copper artificial nacre fabricated by a preform impregnation process: bioinspired strategy for strengthening-toughening of metal matrix composite. *ACS Nano* 2015;**9**:6934–43.
41. Zhang D, Zhan Z. Strengthening effect of graphene derivatives in copper matrix composites. *J Alloys Compd* 2016;**654**: 226–33.
42. Chen B, Kondoh K, Imai H et al. Simultaneously enhancing strength and ductility of carbon nanotube/aluminum composites by improving bonding conditions. *Scr Mater* 2016; **113**:158–62.
43. George R, Kashyap KT, Raw R et al. Strengthening in carbon nanotube/aluminum (CNT/Al) composites. *Scr Mater* 2005; **53**:1159–63.
44. He CN, Zhao NQ, Shi CS et al. Mechanical properties and microstructures of carbon nanotube-reinforced Al matrix composite fabricated by in situ chemical vapor deposition. *J Alloys Compd* 2009;**487**:258–62.
45. Kwon H, Estili M, Takagi K et al. Combination of hot extrusion and spark plasma sintering for producing carbon nanotube reinforced aluminum matrix composites. *Carbon* 2009; **47**:570–77.
46. Zhang X, Zhao N, He C. The superior mechanical and physical properties of nanocarbon reinforced bulk composites achieved by architecture design – a review. *Prog Mater Sci* 2020;**113**:100672.
47. Zhao Z, Bai P, Du W et al. An overview of graphene and its derivatives reinforced metal matrix composites: preparation, properties and applications. *Carbon* 2020;**170**:302–26.
48. Montazeri A, Mobarghei A. Nanotribological behavior analysis of graphene/metal nanocomposites via MD simulations: new concepts and underlying mechanisms. *J Phys Chem Solids* 2018;**115**:49–58.
49. Sosso GC, Chen J, Cox SJ et al. Crystal nucleation in liquids: open questions and future challenges in molecular dynamics simulations. *Chem Rev* 2016;**116**:7078–116.
50. Klepeis JL, Lindorff-Larsen K, Dror RO et al. Long-timescale molecular dynamics simulations of protein structure and function. *Curr Opin Struct Biol* 2009;**19**:120–27.
51. Discher DE, Ortiz V, Srinivas G et al. Emerging applications of polymersomes in delivery: from molecular dynamics to shrinkage of tumors. *Prog Polym Sci* 2007;**32**:838–57.
52. Wolf D, Yamakov V, Phillpot SR et al. Deformation of nanocrystalline materials by molecular-dynamics simulation: relationship to experiments? *Acta Mater* 2005;**53**:1–40.
53. Karplus M, McCammon JA. Molecular dynamics simulations of biomolecules. *Nat Struct Biol* 2002;**9**:646–52.
54. Wang PJ, Cao Q, Wang HP et al. Fivefold enhancement of yield and toughness of copper nanowires via coating carbon nanotubes. *Nanotechnology* 2020;**31**:115703.
55. Tsai PC, Jeng YR. Experimental and numerical investigation into the effect of carbon nanotube buckling on the

reinforcement of CNT/Cu composites. *Compos Sci Technol* 2013;**79**:28–34.
56. Pal S, Babu PN, Gargeya BSK et al. Molecular dynamics simulation based investigation of possible enhancement in strength and ductility of nanocrystalline aluminum by CNT reinforcement. *Mater Chem Phys* 2020;**243**:122593.
57. Suk ME. Enhanced tensile properties of weight-reduced nanoporous carbon nanotube-aluminum composites. *Mater Express* 2019;**9**:801–07.
58. Suk ME. Atomistic behavior of nanoporous carbon nanotube-aluminum composite under compressive loading. *Mater Res Express* 2020;**7**:015028.
59. Kumar S. Graphene engendered aluminum crystal growth and mechanical properties of its composite: an atomistic investigation. *Mater Chem Phys* 2018;**208**:41–48.
60. Kumar S, Pattanayek SK, Das SK. Reactivity-controlled aggregation of graphene nanoflakes in aluminum matrix: atomistic molecular dynamics simulation. *J Phys Chem C* 2019;**123**:18017–27.
61. Kumar S. Graphene engendered 2-D structural morphology of aluminum atoms: molecular dynamics simulation study. *Mater Chem Phys*, 2017;**202**:329–39.
62. Duan K, Li L, Hu Y et al. Interface mechanical properties of graphene reinforced copper nanocomposites. *Mater Res Express* 2017;**4**:115020.
63. Choi BK, Yoon GH, Lee S. Molecular dynamics studies of CNT-reinforced aluminum composites under uniaxial tensile loading. *Compos B Eng* 2016;**91**:119–25.
64. Tsai P-C, Jeng Y-R. Enhanced mechanical properties and viscoelastic characterizations of nanonecklace-reinforced carbon nanotube/copper composite films. *Appl Surf Sci* 2015;**326**:131–38.
65. Silvestre N, Faria B, Lopes JN. Compressive behavior of CNT-reinforced aluminum composites using molecular dynamics. *Compos Sci Technol* 2014;**90**:16–24.
66. Dixit S, Mahata A, Mahapatra DR et al. Multi-layer graphene reinforced aluminum—manufacturing of high strength composite by friction stir alloying. *Compos B Eng* 2018;**136**:63–71.
67. Hou D, Lu Z, Li X et al. Reactive molecular dynamics and experimental study of graphene-cement composites: structure, dynamics and reinforcement mechanisms. *Carbon* 2017;**115**:188–208.
68. Moghadam AD, Omrani E, Menezes PL et al. Mechanical and tribological properties of self-lubricating metal matrix nanocomposites reinforced by carbon nanotubes (CNTs) and graphene—a review. *Compos B Eng* 2015;**77**:402–20.
69. Chen SJ, Li CY, Wang Q et al. Reinforcing mechanism of graphene at atomic level: friction, crack surface adhesion and 2D geometry. *Carbon* 2017;**114**:557–65.
70. Giannozzi P, Baroni S, Bonini N et al. QUANTUM ESPRESSO: a modular and open-source software project for quantum simulations of materials. *J Phys Condens Matter* 2009;**21**:395502.
71. Phillips JC, Braun R, Wang W et al. Scalable molecular dynamics with NAMD. *J Comput Chem* 2005;**26**:1781–802.
72. Plimpton S. Fast parallel algorithms for short-range molecular-dynamics. *J Comput Phys* 1995;**117**:1–19.
73. Song HY, Li YL, An MR. Atomic simulations of the effect of twist grain boundaries on deformation behavior of nanocrystalline copper. *Comput Mater Sci* 2014;**84**:40–44.
74. Yu Q, Li S, Minor AM et al. High-strength titanium alloy nanopillars with stacking faults and enhanced plastic flow. *Appl Phys Lett* 2012;100:063109.
75. Chen J-L, Hsieh J-Y, Chang J-G et al. Molecular dynamical investigation on dislocation near twist-grain boundary of Ni under compression. *J Appl Phys* 2011;**110**:094315.
76. Trautt ZT, Adland A, Karma A et al. Coupled motion of asymmetrical tilt grain boundaries: molecular dynamics and phase field crystal simulations. *Acta Mater* 2012;**60**:6528–46.
77. Zhang RF, Germann TC, Wang J et al. Role of interface structure on the plastic response of Cu/Nb nanolaminates under shock compression: non-equilibrium molecular dynamics simulations. *Scr Mater* 2013;**68**:114–17.
78. Sansoz F, Molinari J F. Mechanical behavior of Sigma tilt grain boundaries in nanoscale Cu and Al: a quasicontinuum study. *Acta Mater* 2005;**53**:1931–44.
79. Pan Y, Adams BL, Olson T et al. Grain-boundary structure effects on intergranular stress corrosion cracking of Alloy X-750. *Acta Mater* 1996;**44**:4685–95.
80. Alder BJ, Wainwright TE. Phase transition for a hard sphere system. *J Chem Phys* 1957;**27**:1208–09.
81. Daw MS, Baskes MI. Embedded-atom method: derivation and application to impurities, surfaces, and other defects in metals. *Phys Rev B Condens Matter* 1984;**29**:6443–53.
82. Dandekar CR, Shin YC. Molecular dynamics based cohesive zone law for describing Al–SiC interface mechanics. *Compos Part A Appl Sci Manuf* 2011;**42**:355–63.
83. Stuart SJ, Tutein AB, Harrison JA. A reactive potential for hydrocarbons with intermolecular interactions. *J Chem Phys* 2000;**112**:6472–86.
84. Tersoff J. New empirical approach for the structure and energy of covalent systems. *Phys Rev B Condens Matter* 1988;**37**:6991–7000.
85. Wang JF, Xie HQ. Molecular dynamic investigation on the structures and thermal properties of carbon nanotube interfaces. *Appl Therm Eng* 2015;**88**:347–52.
86. Zhang C, Lu C, Pei LQ et al. Molecular dynamics simulation of the negative Poisson's ratio in graphene/cu nanolayered composites: implications for scaffold design and telecommunication cables. *ACS Appl Nano Mater* 2020;**3**:496–505.
87. Sidorenkov AV, Kolesnikova SV, Saletsky AM. Molecular dynamics simulation of graphene on Cu (111) with different Lennard-Jones parameters. *Eur Phys J B* 2016;89.
88. Tsai PC, Jeng YR. Coalescence and epitaxial self-assembly of Cu nanoparticles on graphene surface: a molecular dynamics study. *Comput Mater Sci* 2019;**156**:104–10.
89. Maekawa K, Itoh A. Friction and tool wear in nano-scale machining—a molecular-dynamics approach. *Wear* 1995;**188**:115–22.
90. Peng WX, Sun K, Abdullah R et al. Strengthening mechanisms of graphene coatings on Cu film under nanoindentation: a molecular dynamics simulation. *Appl Surf Sci* 2019;**487**:22–31.
91. Nielson KD, Duin AV, Oxgaard J et al. Development of the ReaxFF reactive force field for describing transition metal catalyzed reactions, with application to the initial stages of the catalytic formation of carbon nanotubes. *J Phys Chem A* 2005;**109**:493–99.
92. Bejagam KK, Singh S, Deshmukh SA. Nanoparticle activated and directed assembly of graphene into a nanoscroll. *Carbon* 2018;**134**:43–52.
93. Zhang C, van Duin ACT, Seo JW et al. Weakening effect of nickel catalyst particles on the mechanical strength of the carbon nanotube/carbon fiber junction. *Carbon* 2017;**115**:589–99.
94. Xiang J, Xie L, Meguid SA et al. An atomic-level understanding of the strengthening mechanism of aluminum matrix

composites reinforced by aligned carbon nanotubes. *Comput Mater Sci* 2017;**128**:359–72.
95. Yan Y, Lei Y, Liu S. Tensile responses of carbon nanotubes-reinforced copper nanocomposites: molecular dynamics simulation. *Comput Mater Sci* 2018;**151**:273–77.
96. Srivastava A K, Mokhalingam A, Singh A et al. Molecular dynamics study of mechanical properties of carbon nanotube reinforced aluminum composites. In: *International Conference on Condensed Matter and Applied Physics* (Icc 2015), Bikaner, India. 2016, p. 1728.
97. Patel PR, Sharma S, Tiwari SK. Molecular dynamics simulation for interfacial properties of carbon nanotube reinforced aluminum composites. *Modelling Simul Mater Sci Eng* 2021;**29**: 015004.
98. Jagannatham M, Chandran P, Sankaran S et al. Tensile properties of carbon nanotubes reinforced aluminum matrix composites: a review. *Carbon* 2020;**160**:14–44.
99. Park DM, Kim JH, Lee SJ et al. Analysis of geometrical characteristics of CNT-Al composite using molecular dynamics and the modified rule of mixture (MROM). *J Mech Sci Technol* 2018;**32**:5845–53.
100. Awad I, Ladani L. Molecular dynamics simulation of mechanical interface behavior of copper and single walled carbon nanotube bundles. In: *Proceedings of the Asme International Mechanical Engineering Congress and Exposition*, Montreal, Canada. 2014, Vol. 10, 2015.
101. Patel PR, Sharma S, Tiwari SK. A molecular dynamics investigation for predicting the effect of various parameters on the mechanical properties of carbon nanotube-reinforced aluminum nanocomposites. *J Mol Model* 2020;**26**:238.
102. Babu PN, Gargeya BSK, Ray BC et al. Atomistic investigation of mechanical behavior for CNT reinforced nanocrystalline aluminum under biaxial tensile loading. *Mater Today Proc* 2020;**33**:4942–50.
103. Faria B, Guarda C, Silvestre N et al. Strength and failure mechanisms of CNT-reinforced copper nanocomposite. *Compos B Eng* 2018;**145**:108–20.
104. Inoue S, Matsumura Y. Molecular dynamics simulation of physical vapor deposition of metals onto a vertically aligned single-walled carbon nanotube surface. *Carbon* 2008;**46**: 2046–52.
105. Inoue S, Matsumura Y. Influence of metal coating on single-walled carbon nanotube: molecular dynamics approach to determine tensile strength. *Chem Phys Lett* 2009;**469**:125–29.
106. Shibuta Y, Maruyama S. Bond-order potential for transition metal carbide cluster for the growth simulation of a single-walled carbon nanotube. *Comput Mater Sci* 2007;**39**:842–48.
107. He Y, Huang F, Li H et al. Tensile mechanical properties of nano-layered copper/graphene composite. *Physica E Low Dimens Syst Nanostruct* 2017. **87**:233–36.
108. Wang X, Wang XL, Wang Z et al. Thermal transport across Cu-Metal-Carbon nanotube interfaces enhanced by effective interfacial interaction. *Chem Phys* 2021;**542**: 111019.
109. Duan K, Li L, Hu Y et al. Enhanced interfacial strength of carbon nanotube/copper nanocomposites via Ni-coating: molecular-dynamics insights. *Physica E Low Dimens Syst Nanostruct* 2017;**88**:259–64.
110. Nasiri S, Wang K, Yang M J et al. Nickel coated carbon nanotubes in aluminum matrix composites: a multiscale simulation study. *Eur Phys J B* 2019;**92**:196.
111. Zhou X, Liu XX, Sansoz F et al. Molecular dynamics simulation on temperature and stain rate-dependent tensile response and failure behavior of Ni-coated CNT/Mg composites. *Appl Phys S* 2018;**124**:506.
112. Hidalgo-Manrique P, Lei X, Xu R et al. Copper/graphene composites: a review. *J Mater Sci* 2019;**54**:12236–89.
113. Yang M, Liu Y, Fan T et al. Metal-graphene interfaces in epitaxial and bulk systems: a review. *Prog Mater Sci* 2020;**110**: 100652.
114. Hua J, Duan ZR, Song C et al. Molecular dynamics study on the tensile properties of graphene/Cu nanocomposite. *Int J Comput Mater Sci Eng* 2017;**6**:1750021.
115. Zhang J, Xu Q, Gao L et al. A molecular dynamics study of lubricating mechanism of graphene nanoflakes embedded in Cu-based nanocomposite. *Appl Surf Sci* 2020;511:145620.
116. Liu X, Wang F, Wang W et al. Interfacial strengthening and self-healing effect in graphene-copper nanolayered composites under shear deformation. *Carbon* 2016;**107**:680–88.
117. Weng SY, Ning HM, Fu T et al. Molecular dynamics study of strengthening mechanism of nanolaminated graphene/Cu composites under compression. *Sci Rep* 2018;**8**:3089.
118. Rong Y, He HP, Zhang L et al. Molecular dynamics studies on the strengthening mechanism of Al matrix composites reinforced by grapnene nanoplatelets. *Comput Mater Sci* 2018; **153**:48–56.
119. Duan K, Zhu F, Tang K et al. Effects of chirality and number of graphene layers on the mechanical properties of graphene-embedded copper nanocomposites. *Comput Mater Sci* 2016;**117**:294–99.
120. Zhu FL, Duan K, He LP et al. Effects of chirality and position of graphene on the bending properties of graphene-embedded copper nanocomposites. *J Nanosci Nanotechnol* 2017;**17**: 3105–10.
121. Zhao H, Min K, Aluru NR. Size and chirality dependent elastic properties of graphene nanoribbons under uniaxial tension. *Nano Lett* 2009;**9**:3012–15.
122. Zhang C, Lu C, Pei LQ et al. The negative Poisson's ratio and strengthening mechanism of nanolayered graphene/Cu composites. *Carbon* 2019;**143**:125–37.
123. Zhang S, Xu YF, Liu XY et al. Competing roles of interfaces and matrix grain size in the deformation and failure of polycrystalline Cu-graphene nanolayered composites under shear loading. *Phys Chem Chem Phys* 2018;**20**:23694–701.
124. Mokhalingam A, Kumar D, Srivastava A. Mechanical behavior of graphene reinforced aluminum nano composites. *Mater Today* 2017;**4**:3952–58.
125. Muller SE, Santhapuram RR, Nair AK. Failure mechanisms in pre-cracked Ni-graphene nanocomposites. *Comput Mater Sci* 2018;**152**:341–50.
126. Zhao YX, Liu XY, Zhu J et al. Unusually high flexibility of graphene-Cu nanolayered composites under bending. *Phys Chem Chem Phys* 2019;**21**:17393–99.
127. Rezaei R. Tensile mechanical characteristics and deformation mechanism of metal-graphene nanolayered composites. *Comput Mater Sci* 2018;**151**:181–88.
128. Zhu JQ, Yang QS, He XQ et al. Micro-mechanism of interfacial separation and slippage of graphene/aluminum nanolaminated composites. *Nanomaterials* 2018;**8**:1046.
129. Li L, Sun R, Zhang Y et al. Mechanical behaviors of graphene reinforced copper matrix nanocomposites containing defects. *Comput Mater Sci* 2020;**182**:109759.
130. Zhao G, Li X, Huang M et al. The physics and chemistry of graphene-on-surfaces. *Chem Soc Rev* 2017;**46**:4417–49.
131. Rezaei R, Deng C, Tavakoli-Anbaran H et al. Deformation twinning-mediated pseudoelasticity in metal-graphene nanolayered membrane. *Philos Mag Lett* 2016;**96**:322–29.
132. Zhou XH, Liu X, Lei J et al. Atomic simulations of the formation of twist grain boundary and mechanical properties of

graphene/aluminum nanolaminated composites. *Comput Mater Sci* 2020;**172**:109342.
133. Charleston J, Agrawal A, Mirzaeifar R. Effect of interface configuration on the mechanical properties and dislocation mechanisms in metal graphene composites. *Comput Mater Sci*, 2020;**178**:109621.
134. Agrawal A, Mirzaeifar R. Copper-graphene composites; developing the MEAM potential and investigating their mechanical properties. *Comput Mater Sci* 2021;**188**:110204.
135. Long X J, Li B, Wang L et al. Shock response of Cu/graphene nanolayered composites. *Carbon*, 2016. **103**:457–63.
136. Hwang B, Kim W, Kim J et al. Role of graphene in reducing fatigue damage in Cu/Gr Nanolayered Composite. *Nano Lett* 2017;**17**:4740–45.
137. Montazeri A, Panahi B. MD-based estimates of enhanced load transfer in graphene/metal nanocomposites through Ni coating. *Appl Surf Sci* 2018;**457**:1072–80.
138. Han RQ, Song HY, Wang JY et al. Strengthening mechanism of Al matrix composites reinforced by nickel-coated graphene: insights from molecular dynamics simulation. *Phys B Condens Matter* 2021;**601**:412620.
139. Kinloch IA, Suhr J, Lou J et al. Composites with carbon nanotubes and graphene: an outlook. *Science* 2018;**362**:547–53.
140. Georgakilas V, Otyepka M, Bourlinos AB et al. Functionalization of graphene: covalent and non-covalent approaches, derivatives and applications. *Chem Rev* 2012;**112**:6156–214.
141. Zheng Q, Geng Y, Wang S et al. Effects of functional groups on the mechanical and wrinkling properties of graphene sheets. *Carbon* 2010;**48**:4315–22.
142. Zhao S, Zhang Y, Yang J et al. Significantly improved interfacial shear strength in graphene/copper nanocomposite via wrinkles and functionalization: a molecular dynamics study. *Carbon* 2021;**174**:335–44.
143. He HP, Rong Y, hang L. Molecular dynamics studies on the sintering and mechanical behaviors of graphene nanoplatelet reinforced aluminum matrix composites. *Modelling Simul Mater Sci Eng* 2019;**27**:065006.
144. Zhang YH, An Q, Li JJ et al. Strengthening mechanisms of graphene in copper matrix nanocomposites: a molecular dynamics study. *J Mol Model* 2020;**26**:335.
145. Peng WX, Sun K, Zhang M et al. Effects of graphene coating on the plastic deformation of single crystal copper nano-cuboid under different nanoindentation modes. *Mater Chem Phys* 2019;**225**:1–7.
146. Peng WX, Sun K. Effects of Cu/graphene interface on the mechanical properties of multilayer Cu/graphene composites. *Mech Mater* 2020;**141**:103270.
147. Lei YX, Yan YP, Lv JJ. Atomistic study of the strengthening mechanisms of graphene coated aluminum. *Nanotechnology* 2020;**31**:055708
148. Yan Y, Zhou S, Liu S. Atomistic simulation on nanomechanical response of indented graphene/nickel system. *Comput Mater Sci* 2017;**130**:16–20.
149. Yang ZY, Wang DD, Lu ZX et al. Atomistic simulation on the plastic deformation and fracture of bio-inspired graphene/Ni nanocomposites. *Appl Phys Lett* 2016;**109**:191909.
150. Zhang S, Huang P, Wang F. Graphene-boundary strengthening mechanism in Cu/graphene nanocomposites: a molecular dynamics simulation. *Mater Des* 2020;**190**:108555.
151. Faria B, Guarda C, Silvestre N et al. Aluminum composites reinforced by gamma-graphynes: the effect of nanofillers porosity and shape on crystal growth and composite strengthening. *Comput Mater Sci* 2020;**176**:109538.
152. Zhu JQ, Liu X, Yang QS. Dislocation-blocking mechanism for the strengthening and toughening of laminated graphene/Al composites. *Comput Mater Sci* 2019;**160**:72–81.
153. Zhou Y, Jiang WG, Feng XQ et al. In-plane compressive behavior of graphene-coated aluminum nano-honeycombs. *Comput Mater Sci* 2019;**156**:396–403.
154. Zhou XH, Liu X, Shang JJ et al. Grain-size effect on plastic flow stress of nanolaminated polycrystalline aluminum/graphene composites. *Mech Mater* 2020;**148**:103530.
155. Shuang F, Aifantis KE. Dislocation-graphene interactions in Cu/graphene composites and the effect of boundary conditions: a molecular dynamics study. *Carbon* 2021;**172**:50–70.
156. Zhang X, Xu Y, Wang M et al. A powder-metallurgy-based strategy toward three-dimensional graphene-like network for reinforcing copper matrix composites. *Nat Commun* 2020;**11**:2775.
157. Parsapour H, Ajori S, Ansari R. A molecular dynamics study on the tensile characteristics of various metallic glass nanocomposites reinforced by Weyl semimetals three-dimensional graphene network. *Eur J Mech A-Solids* 2021;**85**:104104.
158. Duan K, Li L, Hu YJ et al. Interface mechanical properties of graphene reinforced copper nanocomposites. *Mater Res Express* 2017;**4**:115020
159. Sharma S, Kumar P, Chandra R. Mechanical and thermal properties of graphene-carbon nanotube-reinforced metal matrix composites: a molecular dynamics study. *J Compos Mater* 2017;**51**:3299–313.
160. Bashirvand S, Montazeri A. New aspects on the metal reinforcement by carbon nanofillers: a molecular dynamics study. *Mater Des* 2016;**91**:306–13.
161. Sanchez-Lengeling B, Aspuru-Guzik A. Inverse molecular design using machine learning: generative models for matter engineering. *Science* 2018;**361**:360–65.
162. Ward L, Liu R, Krishna A et al. Including crystal structure attributes in machine learning models of formation energies via Voronoi tessellations. *Phys Rev B* 2017;**96**:024104.
163. Sun WB, Zheng YJ, Yang K et al. Machine learning-assisted molecular design and efficiency prediction for high-performance organic photovoltaic materials. *Sci Adv* 2019;**5**:eaay4275